STRUCTURAL INVESTIGATION OF TRANSGLUTAMINASES

ATTILA AMBRUS

PH. D. DISSERTATION

SUPERVISOR: PROF. DR. LÁSZLÓ FÉSÜS

University of Debrecen
Department of Biochemistry and Molecular Biology
DEBRECEN

2001

1. CONTENTS

2. ABBREVIATIONS

ATP	-	adenosine triphosphate
BSA	-	bovine serum albumine
CPMG-sequence	-	Carr-Purcell-Meiboom-Gill pulse-sequence for T_2-determinations
e	-	electron charge
EDTA	-	ethylene diamine tetraacetic acid
ELISA	-	enzyme linked immuno sorbent assay
$[E]_0$	-	initial (total) concentration of the enzyme
GST-HTG2	-	GST-fused recombinant human TGase 2
GTP	-	guanosine triphosphate
h	-	Planck constant
I	-	nuclear spin
K_d	-	dissociation constant
η	-	asymmetry parameter
$[M]_0$	-	initial (total) concentration of the metal ion
n	-	number of binding sites
NMR	-	nuclear magnetic resonance
OD	-	optical density
p	-	molar fraction of a particle
PEG	-	polyethylene glycol
PMSF	-	phenyl methyl sulphonyl fluoride
Q	-	nuclear quadrupole moment
q_{zz}	-	electric field gradient
R	-	relaxation rate (=1/T)
rpm	-	rotation per minute
SDS-PAGE	-	sodium dodecyl sulfate polyacrylamide gel electrophoresis
τ_c	-	global reorientational correlation time
TG(ase)	-	transglutaminase
Tris	-	Tris(hydroximethyl)aminomethane
Triton X	-	t-Octylphenoxy polyethoxy ethanol
tTGase	-	tissue TGase (TGase 2)
T_1	-	spin-lattice relaxation time
T_2	-	spin-spin relaxation time
T_{2B}	-	T_2 of the protein-bound metal ion
T_{2F},	-	T_2 of the (protein-free) metal ion
T_{2obs}	-	observed overall T_2
χ	-	quadrupolar coupling constant
$\nu_{1/2}$	-	observed line width at half-height

3. INTRODUCTION

3.1. Transglutaminases in general

Transglutaminases are Ca^{2+}-dependent acyltransferases that catalyze the formation of amide bonds between the γ–carboxamide groups of peptide-bound glutamine residues and the primary amino groups of different amines including the ε–amino groups of lysine side-chains in proteins.

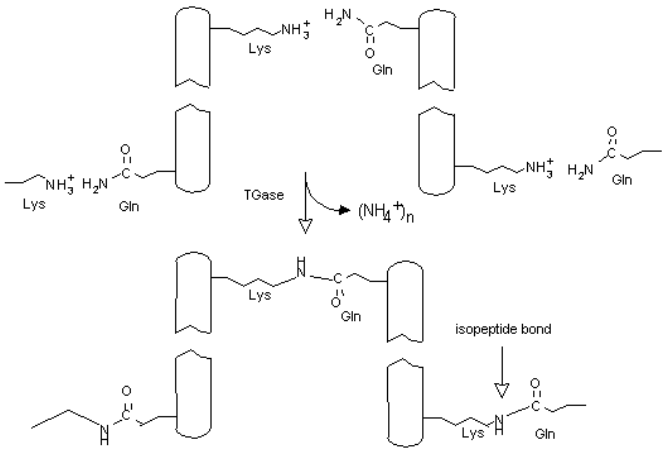

Figure 1. The transglutaminase reaction.

For understanding the TGase reaction, the most critical data are related to the Ca^{2+} activation processes of these enzymes.

Several TGases are identified and characterized. These are the following: FXIII, TGase 1-5 and Band 4.2. TGase 1 crosslinks structural proteins during epidermal differentiation [1]; TGase 4 is a hormone-mediated extracellular enzyme having a role in the seminal fluid production [2]; TGase 5 (or TGase X) is present in two alternative forms in keratinocytes showing wide expression patterns in both growing and adult organisms [3]; Band 4.2 is a cytoskeletal protein which lost its TGase activity and works as a structural protein in eritroid cells [4]. Although, we have more and more insights into the

physiological roles of all the above mentioned enzymes, the most widely investigated TGases are still the FXIII, TGase 2 and TGase 3.

3.2. Human Factor XIII

Two forms of FXIII exist. The plasma enzyme contains two A and two B subunits together in a heterotetramer while the cellular enzyme consists of two identical A subunits [5]. The plasma coagulation factor XIII is the last enzyme in the blood coagulation cascade stabilizing the fibrin soft clot making it unsusceptible to fibrinolysis by crosslinking fibrin and/or α_2-antiplasmin (the inhibitor of plasmin) onto the clot. The function of the cellular enzyme is still obscure. The structure of the cellular zymogen has been solved at 2.1Å resolution by X-ray crystallography as shown on Figure 2 [6].

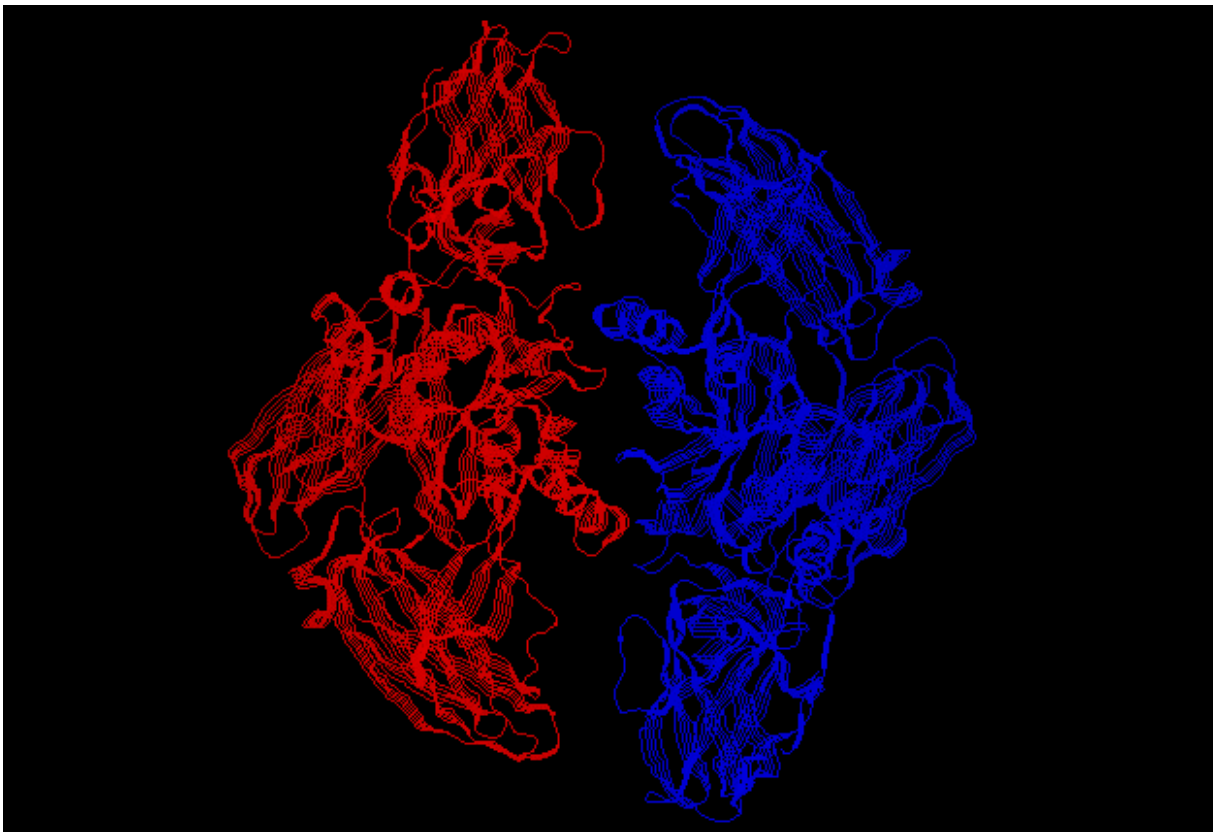

Figure 2. The highest resolution structure of FXIII-A_2.

^{43}Ca NMR studies have elucidated that the B subunit does not bind Ca^{2+} [7]. The X-ray studies also showed that each A subunit binds one Ca^{2+} with high affinity causing very small conformational changes (even in the proximal area of the binding site) [8] while equilibrium dialysis suggested two tightly bound Ca^{2+}s and up to six more with smaller affinities on the FXIII-A_2B_2 tetramer at slightly higher Ca^{2+} concentrations [9]. The overall Ca^{2+} affinity of plasma FXIII was determined to be Kd≅0.1mM [5, 9]. In physiological conditions, both plasma and cellular FXIII require a proteolytic cleavage (by thrombin) between Arg37 and Gly38 for their activation. However, *in vitro,* in the presence of low Ca^{2+} and high inert salt concentration the cellular FXIII, while at high Ca^{2+} and low salt concentration, both forms of FXIII assume active conformations without any proteolytic cleavage as shown in Figure 3. [5, 10]. There have been no quantitative data on the Ca^{2+} binding properties of FXIIIs under these conditions. Earlier it is elucidated that several divalent and trivalent metal ions except Mg^{2+} can be bound to plasma FXIII [9].

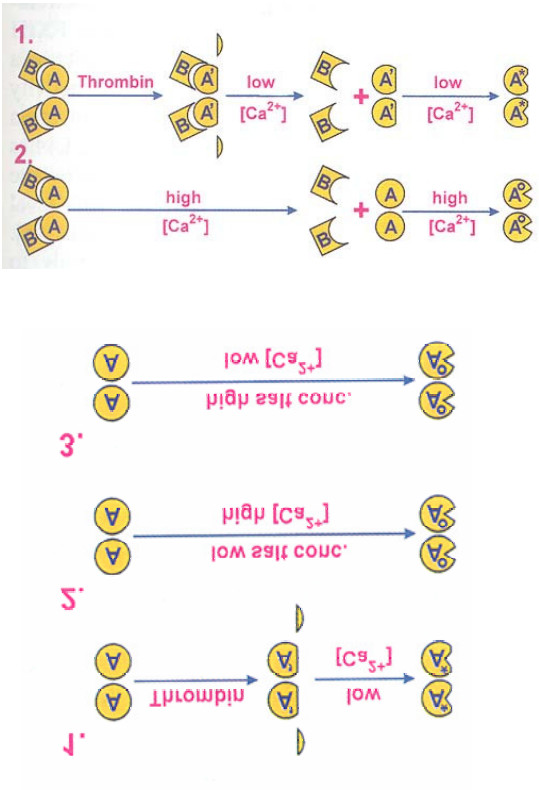

Figure 3. Activation of the plasma and cellular FXIIIs.

3.3. Human TGase 2

The human tissue-type transglutaminase (TGase 2) has been implicated in stimulus secretion coupling [11], receptor mediated endocytosis [12], programmed cell death [13], extracellular matrix organization and cell adhesion [14], cell growth and proliferation [15] and tumor growth [16, 17]. The protein, which is a monomer molecule, could not be crystallized, yet. However, because of homology to FXIII it is possible to build up its homology model.

The Ca^{2+} binding properties of the human TGase 2 molecule were investigated in its purified form and in permeabilized cells [18, 19, 20]. The number of Ca^{2+} binding to one enzyme molecule was estimated to be six by equilibrium dialysis and all binding sites were proposed to be a high affinity site having similar Ca^{2+} affinities giving a hyperbolic saturation curve with an apparent affinity constant of 90μM titrated at low Ca^{2+} concentrations [18]. At higher Ca^{2+} concentrations a "fast-moving" (on SDS gel) form of the human TGase 2 molecule was detected, and the existence of low affinity Ca^{2+} binding sites was proposed without giving their number, localization and affinity constants [19].

GTP lowers the Ca^{2+} affinity and the transamidase activity of human TGase 2 binding to the core domain of the molecule at amino acids 159-173 and causing considerable conformational changes [18, 21]; however it has not been clarified how many and which Ca^{2+} binding sites are affected. The TGase 2 hydrolyses GTP/ATP when they are in the form of their Mg^{2+}-complexes [21]. The GTP binding properties of TGase 2 help it to fulfill its roles in the cytoplasmatic signaling pathways as a G-protein and proves the bifunctional nature of TGase 2 as the two functions (cross-linking and signaling) can be switched on and off by changing the Ca^{2+}/GTP ratio. Ca^{2+} and GTP can also influence the proteolytic and folding behaviors of the enzyme suggesting another level of pharmacological regulation [22, 23].

With its C-terminal eight amino acids TGase 2 is capable of binding phospholipase C while the N-terminal seven residues can be bound to fibronectin representing the broadened repertoire of physiological functions the enzyme possesses.

3.4. Human TGase 3

The monomer TGase 3 is essential in keratinization participating in the formation of the insoluble cornified envelope in the dying keratinocytes [24]. There has been no studies so far regarding its Ca^{2+} binding properties. It is known that the activity of the enzyme is retained in a 50kDa part after

limited proteolysis necessary for its activation [25]; it is likely that this fragment binds Ca^{2+}. Before the proteolytic cleavage, the shape of the molecule is more elongated than that of the other TGases, but after the cleavage, a shrinking effect takes place, which can be an explanation for several behaviors of this enzyme differing from those of other TGases.

3.5. Investigation of proteins by metal NMR

There are several proteins which are already studied by ^{43}Ca, ^{25}Mg and other metal NMR using different theoretical and technical approaches. These methods provide unique and completely ion-specific means of obtaining both qualitative and quantitative information about the metal ion binding proteins (for reviews, see [26, 27]). Using this method, different intracellular Ca^{2+} binding proteins such as calmodulin, troponin C [28-32] and several proteins with much weaker binding capability, e.g. prothrombin [33, 34] and *FXIII-*A_2B_2 [7] were already investigated. Phospholipase A_2 [35] among others [36-48] and even DNA [49-51] could be studied by ^{43}Ca NMR providing valuable pieces of information.

3.6. Folding studies of proteins

There are several factors determine the folding of a protein chain to its final 3D organization. There are intermediate (partially folded) structures produced in folding pathways, some of which possess partial activities and could be isolated because of their stability. The thermodynamic parameters of the folding equilibrium between these intermediates and the final structure determine the stability of the active conformation. Effectors can shift the folding (or unfolding, or refolding) equilibrium towards the production of the active conformation (helper agents, e.g. natural substrates of the enzyme) or against it (unfolding agents, e.g. urea).

During the production of a recombinant protein, we often face to the problem of the solubility of the product. If the amount of the expressed protein in the cytoplasm is not considerable it is very probable that the protein forms so-called *inclusion bodies* in which the desired protein is generally co-precipitated with other proteins binding to each other by Van der Waals forces, hydrogen bonds, salt bridges and even by disulfide bridges. The recovery (refolding) of inclusion body proteins into their active forms has a roughly similar way for all types of protein [52], but there are specific, optimized

recipes for every individual protein because of the differences in their structural properties and the appropriate effector molecules [53-58]. Briefly, the main steps are the following: fermentation, cell lysis and isolation of the inclusion bodies, solubilization of the inclusion bodies, renaturation, purification and characterization of the refolded protein. The development of the successful refolding technique provides the recombinant active protein as well as kinetic and structural data relating to the folding properties of the molecule.

4. OBJECTIVES

Transglutaminases have several physiologically important functions; therefore, detailed structural studies are necessary to clarify the related molecular mechanisms. The above results clearly show that a number of unanswered questions exist about the Ca^{2+} binding properties of the TGases. Therefore, we have decided to initiate a series of ^{43}Ca NMR studies combined with surface polarity analysis and multiple sequence alignment targeting three TGases. We have intended to reveal all the potential Ca^{2+} binding sites of these TGases. The construction of a precise homology model of human TGase 2 was desirable for these purposes. The determination of dissociation constants and binding site symmetry parameters of Ca^{2+} complexes of the enzymes and the ^{25}Mg NMR study of FXIII-A_2 were also considered to be done in the first part of our investigations. Our second focus was related to the elucidation of the Ca^{2+}/GTP effect on folding properties of TGase 2.

5. MATERIALS AND METHODS

5.1. Ca^{2+} binding studies

5.1.1. Preparation of enzymes

The recombinant human TGase 3 and the recombinant human FXIII-A_2 enzyme preparations were the kind gifts of Zoltán Nemes (NIH, Bethesda, Maryland, USA) [59] and Hubert Metzner (Marburg, Germany) [60], respectively. The homemade E.coli construct of the GST-fused human TGase 2 was the gift of Zsolt Keresztessy.

The construction, induction and purification was carried out briefly in the following way: Polymerase chain reaction was carried out with the proof-reading thermostable DNA polymerase, Pfu (Promega) was used to amplify the coding region of the TGase 2 cDNA (Human endotelial cell tissue type TGase gene) for subcloning into the E.coli GST-fusion expression vector pGEX-2T (Amersham Pharmacia Biotech). Oligonucleotide forward primer, 5'CAATTTCACACAGAATTCAGACC**ATG**GCCGAGGAG3', and reverse primer, 5'CCAAAACAGCCAGAATTCGG*TTA*GGCGGGGCCAATG3', were designed to anneal to the original TGase 2 cDNA [61] sense strand between positions 114-148 and to the antisense strand between positions 2219-2184, respectively, to include the translation start codon ATG (bold face) and termination codon TAA (italics) of the original clone, and to incorporate two EcoRI restriction sites (underlined). For the amplification, the mammalian expression vector construct, pSG5-TGase [62] was used as the template. The thermal cycle consisted of a single denaturation step at 95°C for 5min (hot start), 35 cycles of denaturation at 95°C for 1min, annealing at 50°C for 2min, extension at 72 °C for 6min and a single final extension step at 72°C for 10min. The PCR product was digested with EcoRI and cloned in-frame with GST into the EcoRI site of pGEX-2T. The presence of the 2070bp TGase 2 DNA insert was identified by restriction digestion with EcoRI and the correct orientation was proved by double digestion of the construct with SmaI and XbaI. The recombinant vector was designated pGEX-2T-TGaseII. The pGEX-2T-TGaseII construct was electroporated into the E.coli strain DH5α.

An overnight culture of the transformants was diluted 25 times in 1L of LB medium supplemented with 100μg/ml ampicillin and grown to OD_{600} 0.8-1.0 at 37°C. The induction of the expression was performed by adding isopropyl β-D-thiogalactoside (IPTG) at 0.1mM final

concentration and incubating for 6h at 25^{o}C.

The fusion protein was purified from induced cells according to [63] with some modifications. Briefly, cell pellets (6000g, 10min, 4^{o}C) were sonicated (15min, 50% duty cycle at power output 3 with a Soniprep sonicator) in 25ml buffer A (20mM Tris-HCl, 150mM NaCl, 1mM dithiothreitol, 1mM EDTA, and 10% glycerol) containing 1%(v/v) Triton X-100. Cell lyzates were shaken on ice for 30min and centrifuged at 20,000g for 15min at 4^{o}C. The supernatant was diluted 3 times with buffer A minus glycerol and applied onto glutathione-Sepharose 4B packed into a 1x10cm column and pre-equilibrated with buffer A minus glycerol. The beads were washed with 30 bed volumes of buffer A minus glycerol and the GST-fusion protein was eluted with 10mM reduced glutathione in 50mM Tris-HCl, pH8.0.

Protein concentration was determined using the Bradford method [64]. TGase activity was determined by an amine-incorporation assay (ELISA-method) [65]. Active fractions were pooled and concentrated using CentriCon centrifugal concentrator tubes with a MWCO of 30kDa (Amicon). Fusion protein concentrates were analysed on SDS/PAGE [66] and ECL-Western blotting (Pierce) [67] using goat polyclonal IgG\anti-TGase 2 antibody (Upstate Biotechnologies) for the primary immunoreaction, and the VECTASTAIN ABC Reagent (Vector) with the semi-dry blotting technique [68] for visualisation of immunoreactive bands. Average yield of the glutathione-Sepharose 4B-purified GST-fusion protein per litre of culture medium was 400µg and its purity was estimated to be more than 90% by densitometry of Coomassie-stained polyacrylamide gels.

Agarose, Pfu DNA polymerase, deoxyribonucleotides, T4 DNA ligase, EcoRI, SmaI, XbaI restriction endonucleases were purchased from Promega and the oligonucleotide primers from GibcoBRL.

5.1.2. Preparation of NMR samples

In order to determine the approximate values of the 90° pulse, T_1 and T_2 for the two nuclei, 1M $MgCl_2$ and 1M $CaCl_2$ solutions, with natural isotopic abundance (N.A.), were used. For measuring the exact experimental T_2 of the free metal ions in given concentrations, the following solutions were prepared. For Mg^{2+} 10, 20, 30, 40 and 50mM solutions were made containing 1mM ^{25}Mg enrichment (from 0.6M $^{25}MgCl_2$ stock solution made from solid ^{25}MgO dissolving in stoichiometrically equivalent 1M HCl), 5% D_2O (99.99% pure) for field lock in Buffer A (150mM NaCl, 10mM Tris, pH7.5). 600µl total volume of samples was prepared in the absence and presence of protein as well. For Ca^{2+}: 5% D_2O, 1mM $^{43}CaCl_2$ (from a 75mM $^{43}CaCl_2$ stock solution, dissolving solid $^{43}CaCO_3$ in 1M HCl) in

Buffer A giving the final sample volume of 2.5ml. The volume of the samples containing proteins was the same. These samples were titrated with 1M $CaCl_2$ (N.A.) to reach the following concentrations of Ca^{2+}: 1, 11, 21, 31 and 51mM. The precise determination of 90° pulses was carried out by using enriched materials. ^{25}MgO (enriched to 98.81%) and $^{43}CaCO_3$ (enriched to 83.93%) were purchased from the Oak Ridge National Laboratory (USA).

5.1.3. NMR experiments

^{25}Mg NMR experiments were performed at 22.05MHz (360MHz of proton) with a 5mm inverse broad-band probehead on a Bruker AM-360 spectrometer. Typically 256 transients were used in order to obtain good signal to noise ratio for integration. The ^{43}Ca NMR experiments were performed at 33.7MHz (500MHz of proton) on a Bruker DRX-500 spectrometer with a 10mm direct broad-band probehead. Typically 64 or more transients were applied for good signal to noise ratio. T_1 measurements were carried out by inversion recovery experiments using the standard Bruker microprogram. T_2 measurements were carried out by means of the CPMG sequence with the standard Bruker microprogram. The determination of T_2 with the CPMG sequence has a great advantage compared to the usual line-width method. In this case the inhomogenity of the applied magnetic field is excluded. This inhomogenity sometimes can cause 50% of the effect measured, however what is worst is that the effect changes from sample to sample because of the geometry and the quality of the NMR tubes. Temperature was always stable at 300±1K. After all NMR experiments, the protein concentration was determined again.

5.1.4. Evaluation of NMR data

FIDs were analyzed by the Bruker 1D WinNMR program package. The heights and integrals of the peaks were fit to time as single exponentials in Microsoft Excel 5.0. The evaluation of relaxation parameters was also performed by non-linear parameter fitting using a homemade Gauss – Newton – Marquard algorithm. More exponential terms did not provide significantly better fits [69]. For hyperbolic fitting of the relaxation rate dependence on total Ca^{2+} concentration to the theoretical equation, the program Sigmaplot Version 2001 was used with 100 iteration steps. The exact molecular masses of the enzyme molecules were retrieved from the Swissprot database.

5.1.5. Activation of cellular FXIII-A_2 in two different ways

FXIII-A_2 was cleaved by thrombin in 500µl preincubation volume containing 500U(NIH)/ml thrombin (from human plasma, Sigma), 10mM Ca^{2+}, 2.075mg/ml FXIII-A_2 and buffer B (50mM Tris-HCl, pH7.5) for 20min at 37°C [9]. After cleavage it was diluted to 2.5ml. Activation by high concentration of salt was carried out in 2.5ml buffer B containing 5%D_2O, 2.496µM FXIII-A_2, 1M NaCl and 2mM $CaCl_2$ incubating for 90min at 37°C [10]. For the activation by 150mM NaCl and without salt (50mM Tris-HCl) the same preincubation period was inserted, also already in the final volume of measurement.

5.1.6. Inhibition of human TGase 2 with GTP

The human TGase 2 was activated when Ca^{2+} was added to the incubation mixture. To inhibit the activation process, 10mM GTP was added for two hours before starting NMR experiments [70].

5.1.7. Activation of human TGase 3 by dispase

1U/mg (of protein) and 1 U/ml dispase (grade I, Boehringer Mannheim) without extra Ca^{2+} were used for 30min at room temperature (as manufacturer advised).

5.1.8. TGase activity assay

Measurement of TGase activity was carried out by an amine-incorporation assay in an ELISA plate [65] in which a biotynylated amine substrate was incorporated into dimethylated-casein coated onto the surface. The color reaction was developed by a streptavidin-conjugated alkaline-phosphatase. All samples were prepared as for the NMR experiments and were diluted 4 times in the activation mixture except at the activation of FXIII-A_2 with 1M NaCl, since there a ten-fold dilution factor was applied.

5.1.9. Multiple sequence alignment

The multiple sequence alignment of TGases was created by the GCG program [71] PILEUP and FASTA [72].

5.1.10. Homology modeling

In order to construct the homology model of human TGase 2 using the refined highest resolution structure of FXIII as a template [6], all known primary structures of TGases and related proteins were identified as a first step using the program package GCG. With the GCG program STRINGSEARCH and the search term 'transglutaminase', all TGase sequences from the GENEMBL database were retrieved and with the GCG program FASTA and the sequence of TGase 2, all homologous sequences from the SWISSPROT data base were identified. Pairwise alignments were constructed using BESTFIT. Structure alignments were carried out using the UCLA Fold Prediction server [73]. From the comparison of the alignments, highly conserved regions of the sequences were identified and distinguished from the less-conserved regions. Using the program "O" [74], the side chains of factor XIII-A were replaced in the conserved regions with the corresponding ones of the TGase 2 sequence. The less-conserved regions were deleted and rebuilt by homologous sequences retrieved from a database of known structures. Energy minimizations were carried out using the program XPLOR [75]. The first rounds were calculated without electrostatic potential and explicit hydrogen atoms in order to eliminate the worst close contacts between atoms. In later rounds, electrostatic energy as well as polar hydrogen atoms were included. After each round, a superposition of the model was calculated onto the starting structure of factor XIII using the program LSQKAB of the CCP4 program suite [76]. For structure validation, the program PROCHECK [77] was used. All bond lengths and bond angles that deviated too much from their ideal values were checked manually and adjusted where it was possible. Potential hydrogen bonds and salt bridges were identified. The presumably conserved active center geometry was restrained during the final energy minimization rounds. The representation of the model was made by the program WebLab ViewerPro Version 3.7 (MSI).

5.1.11. Surface polarity analysis

The calculations were made by the program GRASP [78] using the recently determined 3D structure of FXIII-A zymogen [6] and our homology model of TGase 2. Both molecules were probed using the same intensity level of color (red=19.73, blue=14.37).

5.2. Refolding studies

5.2.1. Preparation of inclusion bodies

The E.coli plasmid of the non-fused human TGase 2 was the kind gift of Bruna Pucci (Rome, Italy). After the optimization of the procedure, the plasmid expression was carried out in LB Broth Base containing 100 μg/ml ampicillin at 37 ^{o}C. Expression was initiated at OD=0.5 by adding 1mM IPTG for 105min. The culture was centrifuged (4 ^{o}C, 500 g, 15 min) and homogenized vigorously at 4^{o}C in 3ml of lysis buffer (50mM Tris, 1mM EDTA, 100mM KCl, 133μM PMSF, pH8.0) per wet gram of bacteria. Sonication was carried out with a Branson Sonifier 450 on ice (duty cycle: 40, output: 6, 3.5min) and the homogenate was centrifuged (12,000g, 4^{o}C, 15min). The pellet was resuspended at room temperature in 5ml 2M urea per wet gram of pellet for 5min. This was followed by a centrifugation (25^{o}C, 12,000g, 15min) and the pellet was kept as the inclusion body preparation.

5.2.2. Electronmicroscopic pictures

The electronmicrographs of the inclusion bodies were made according to Marston et al [52]. Briefly, the samples were fixed by 2% glutaraldehyde and dyed by saturated uranyl acetate at 2^{o}C. The grids were coated with lysine. The samples were used without dehydration and dried on air. The transmission electronmicroscope was a JEOL 100B (1973, Japan).

5.2.3. The optimized procedure

According to our most efficient method, the inclusion bodies were suspended in 1ml 8M urea solution containing 0.1mM PMSF, 10mM cysteine, pH10.7 per wet gram of pellet and homogenized at 37°C for 1h. This step was followed by dilution with 9ml dilution buffer (50mM KH_2PO_4, 1mM $CaCl_2$, 1mM GTP, 2mM $MgCl_2$, 50mM NaCl, 0.11mM cystine, pH10.7) per wet gram of pellet. The mixture was stirred slowly at 37°C for 1h and centrifuged (25°C, 12,000g, 15min). The supernatant was dialyzed against dialysis buffer I (1mM $CaCl_2$, 1mM GTP, 2mM $MgCl_2$, 1mM cysteine, 0.1mM cystine and 5(w/v)% PEG, M_r=8000, pH10.0) at 4°C overnight using a dialysis tube with a molecular weight cut-off 12,000. Volumetric ratio of the supernatant and the buffer was 1:100. Dialysis buffer II was used to dialyze PEG and affectors out from the solution (1mM EDTA, 1mM cysteine, 0.1mM cystine, 0.1M Tris, pH8.5) in an overnight dialysis with the same conditions as above. The refolding was left running for weeks at 4°C.

5.2.4. Optimization of refolding

We used several chemicals besides PEG during optimization of refolding adding them into the dialysis buffer I in the indicated concentrations: 0.5M arginine-hydrochloride, 1M Tris, 33mM CHAPS, 10mg/ml lauryl maltoside, 10% glycerol, 0.1% Triton X-100, 1mg/ml bovine serum albumine (BSA). Guanidinium chloride was also used replacing urea. The effect of Ca^{2+}, GTP and ATP on refolding was studied using 1mM $CaCl_2$, 1mM GTP (+2mM $MgCl_2$), ATP (+2mM $MgCl_2$) [79] and their combinations in dialysis buffer I, II and the phosphate containing dilution buffer instead of 1mM EDTA. The effect of the removal of PEG by dialyzation was examined in all cases in parallel experiments.

5.3. Chemicals

All chemicals were purchased from Sigma (St. Louis, MO) unless otherwise indicated.

6. THEORY OF THE NMR APPROACH

Under normal conditions, the nuclear magnetic relaxation of ^{43}Ca (I=7/2) and ^{25}Mg (I=5/2) is dominated by quadrupolar relaxation. The relaxation rate of quadrupolar nuclei increases by orders of magnitude if the chemical environment is changing, especially the symmetry of the environment [80]. This fact presents the possibility that a small percentage of binding can considerably affect the overall transverse relaxation rate (see below). If the so-called extreme-narrowing and fast-exchange conditions apply to the system, the NMR signal can be described as a single Lorentian-curve, the relaxation drops down by a single exponential and the observed relaxation rate is the weighted average of the relaxation rates of the bound and the free metal ion [69]:

$$R_{2obs}=\pi\nu_{1/2}=p_F R_{2F} + p_B R_{2B} \qquad (1)$$

This equation is the basis for the determination of the unknown concentration of bound metal ion. Since the values of molar fractions of the bound and unbound Ca^{2+} are independent of the ratio of the NMR active isotope present in the system, only the necessary (1mM) concentration of $^{43}Ca^{2+}$ and $^{25}Mg^{2+}$ was applied for the titration of the samples. It is not possible to observe the distinct dissociation steps in the case of TGases since both high and low affinity sites are being occupied almost continuously because of the relatively small differences in the Ca^{2+} affinities [9, 18]. Therefore, it is worth calculating the average K_d for the number of Ca^{2+} binding sites. In order to get a theoretical equation for the determination of average K_d from the titration data, first the p_B must be expressed. It is as follows:

$$p_B=n[E]_0/(K_d + [M]_0) \qquad (2)$$

[7]. Taking into consideration that $p_F \sim 1$, the following hyperbolic equation can be deduced and fitted to the reduced relaxation rate – metal ion concentration titration data-points [7]:

$$\Delta(1/T_2)=[E]_0/(T_{2B}/n(K_d+[M]_0)) \qquad (3)$$

where $\Delta(1/T_2)=(\Delta R=R_{2obs}-R_{2F})=1/T_{2obs}-1/T_{2F}$. K_d and T_{2B}/n can be obtained from the fitting as parameters.

In reference [7] and elsewhere, we could not find the deductions of equation 2 and 3 that is why we performed them to check whether they are really applicable to our given situations (Appendix 1).

The relaxation rate of the bound metal ion can be expressed by the following equation provided that the extreme narrowing condition is fulfilled [69]:

$$R_{1B} = R_{2B} = \frac{3\pi^2}{10}\frac{2I+3}{I^2(2I-1)}\chi^2(1+\frac{\eta^2}{3})\tau_c \qquad (4)$$

Where

$$\chi = e^2 q_{zz} Q/h \qquad (5)$$

Since q_{zz} is the electric field gradient around the nucleus, it strongly depends on the symmetry of the binding site, which binds the Ca^{2+}. $1>\eta>0$ and rarely exceeds 0.5 in Ca^{2+} and Mg^{2+} complexes [69], therefore $(1+ \eta^2/3)\sim1.08$. From this equation, only the product of the correlation time and the quadrupolar coupling constant can be obtained. Therefore, there must be an independent measurement or a good approximation for the correlation time in order to determine χ, which is informative about the symmetry of the Ca^{2+} binding sites in a protein molecule. In EF-hand Ca^{2+} binding motifs, this value is typically around 1MHz [80]. Lower values indicate more symmetrical while higher ones less symmetrical binding sites. From these data, one can draw several structural conclusions especially if the correct structure or a homology model is available**.**

In those cases where a small amount of other Ca^{2+} binding agents were present in the system (like dispase or thrombin), and their concentrations were practically negligible compared to the

concentration of the free cation, we measured and corrected the R_{2obs} with the relaxation rate of the "free" Ca^{2+} measured in the presence of this agent at the same concentration as used with the protein. When TGase 2 was inhibited by GTP, because of the high concentration of GTP (which also binds Ca^{2+}), the ratio of Ca^{2+} bound to GTP was no longer negligible. A modified equation was used, the deduction of which is based on the appropriate modifications of equation 1-3 and the high affinity constant of Ca^{2+} for GTP ($6600M^{-1}$) [81] given to the applied condition (for deduction see Appendix 2):

$$1/T_{2obs} - p_F \, 1/T_{2F} = \frac{([M]_0 - 0.01)[E]_0}{[M]_0 \frac{T_{2B}}{n}(K_d + [M]_0 - 0.01)} + \frac{0.01}{[M]_0 T_{2CaGTP}} \qquad (6)$$

where T_{2CaGTP} is the relaxation time of Ca^{2+} bound to GTP and an unknown fitting parameter.

Since the higher ionic strength does not have a considerable influence on T_{2B} [82], the affinity and the symmetry parameter of the Ca^{2+} binding sites of FXIII-A_2 after the activation by 1M NaCl could be calculated as well.

7. RESULTS AND DISCUSSION

7.1. Ca^{2+}-binding studies

7.1.1. Homology model, surface polarity analysis and multiple sequence alignment

In order to obtain the potential Ca^{2+} binding sites of the examined TGases the homology model of TGase 2, surface polarity analysis and a multiple sequence alignment were produced. The highest resolution 3D X-ray structure of cellular FXIII-A_2 zymogen was available for these manipulations [6].

For the construction of the polarity surface of the TGase 2 molecule, a homology model was generated based on the above-mentioned FXIII structure. After exchanging the corresponding side chains, building the loops and several processing and minimization steps, the final structure contained only 2.2% of the amino acids in disallowed regions of the Ramachandran plot. These residues, however, were fixed in their orientations by salt bridges or strong hydrogen bonds. A superposition of this model to the starting structure of factor XIII-A yielded a root mean square deviation of 1.55Å based on 551 superimposed C (alpha) positions. Our model (Figure 4) contains only slight – but structurally important - differences in distances and angles compared to the previously published ones [84, 85, 86] which are based on lower resolution structures of FXIII. Recently, the X-ray structure of a tissue TGase originating from red sea bream containing 666 residues from the total 695 was published [87]; the resolution of this structure is less than that of the FXIII which our homology model is based on (2.5Å versus 2.1Å). Taking into consideration these data and that the sequence identity of this fish protein to the human analogue is just 43.6%, we can state that our model is still the most precise structure of the human TGase 2.

Using our homology model of TGase 2 and the X-ray structure of FXIII-A, the polarity surfaces of these molecules were built up and compared to each other (Figure 5) in order to find those negatively charged amino acids exposed at the surface (designated with red) and most probably responsible for binding of Ca^{2+}. There are several highly negative regions on both molecules, but more on TGase 2 (Table 1). One of the reasons for it is that the FXIII-A has a dimerization surface and there must be hydrophilic amino acids facing water molecules. The surface polarity analysis clearly identifies the recently published high affinity Ca^{2+} binding site of FXIII-A at Asp438, Glu485 and Glu490 (see Figure 5c)[8].

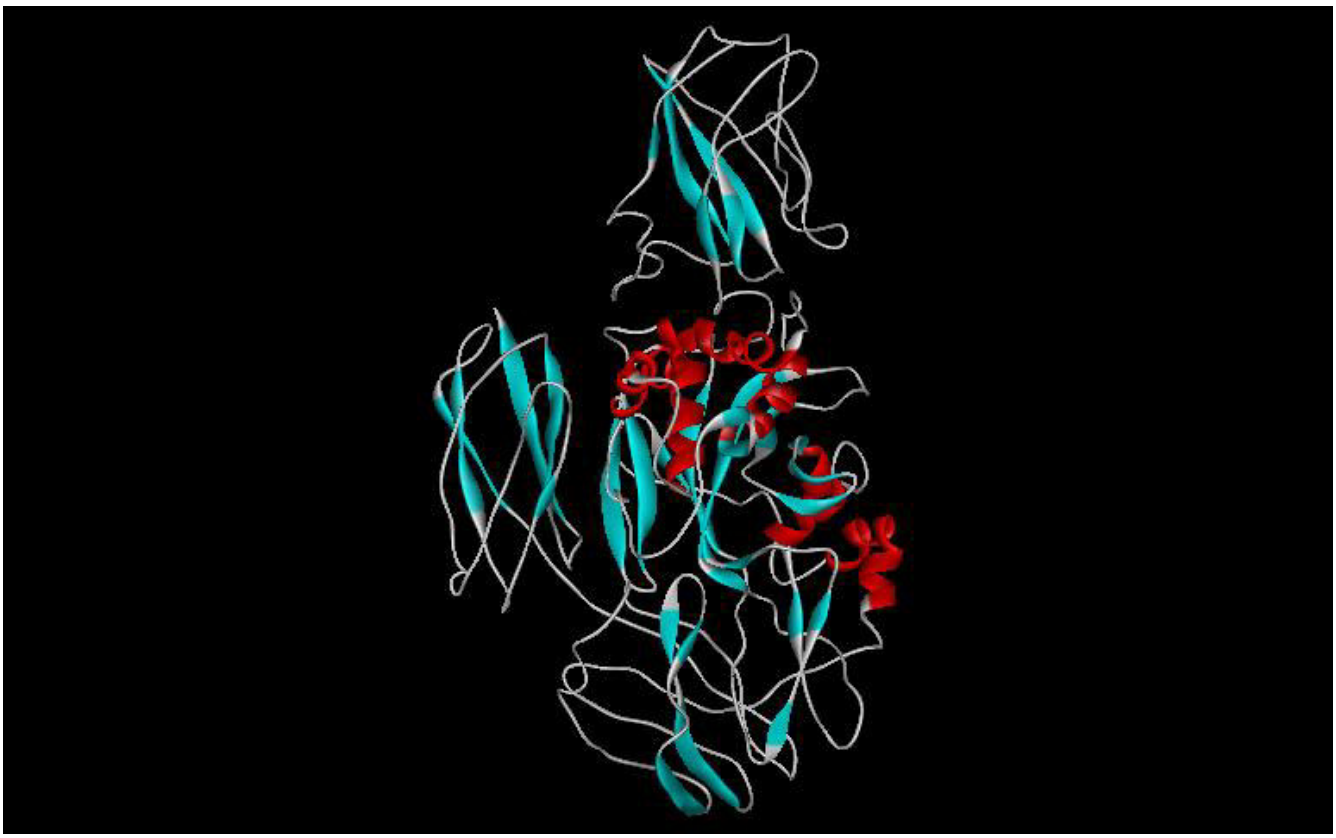

Figure 4. The homology model of the human tissue transglutaminase; it is based on the highest resolution X-ray structure of FXIII-A (2.1Å).

We constructed the multiple sequence alignment of the TGases (Figure 6). Eighteen homologous primary structures were taken into account. The sequence identity of the two other TGases studied here to human TGase 2 according to the program FASTA are the following: human TGase 3 (TGL3_ HUMAN) – human TGase 2 (TGLC_HUMAN) 38.4% and human FXIII-A (F13A_HUMAN) – human TGase 2 (TGLC_HUMAN) 39.0%. Human FXIII-A and human TGase 3 provide 38% of identity to each other. The negatively charged amino acids of the recently determined Ca^{2+} binding site of FXIII (Asp438, Ala 457, Glu485 and Glu490) [8] are well conserved in all TGases. In the alignment, those parts were designated (with yellow) as potential Ca^{2+} binding sites in which the number and density of the negatively charged amino acids were relatively high. The red letters indicate those – originally yellow - sites, which are exposed at the molecular surface according to the surface polarity analysis. This double analysis was carried out only on FXIII-A and TGase 2 since TGase 3 shows big differences in 3D structure from these TGases [25] lowering the possibility of building a reliable homology model. As seen, not all the potential binding sites deduced from the primary sequences

(designated in the alignment with yellow) appeared on the surface as negative clusters for both molecules. Twelve clusters in TGase 2 and five in FXIII-A were identified by both methods (red letters). Beyond these sites, there were more highly negative clusters on polarity-surfaces of both molecules (see Table 1).

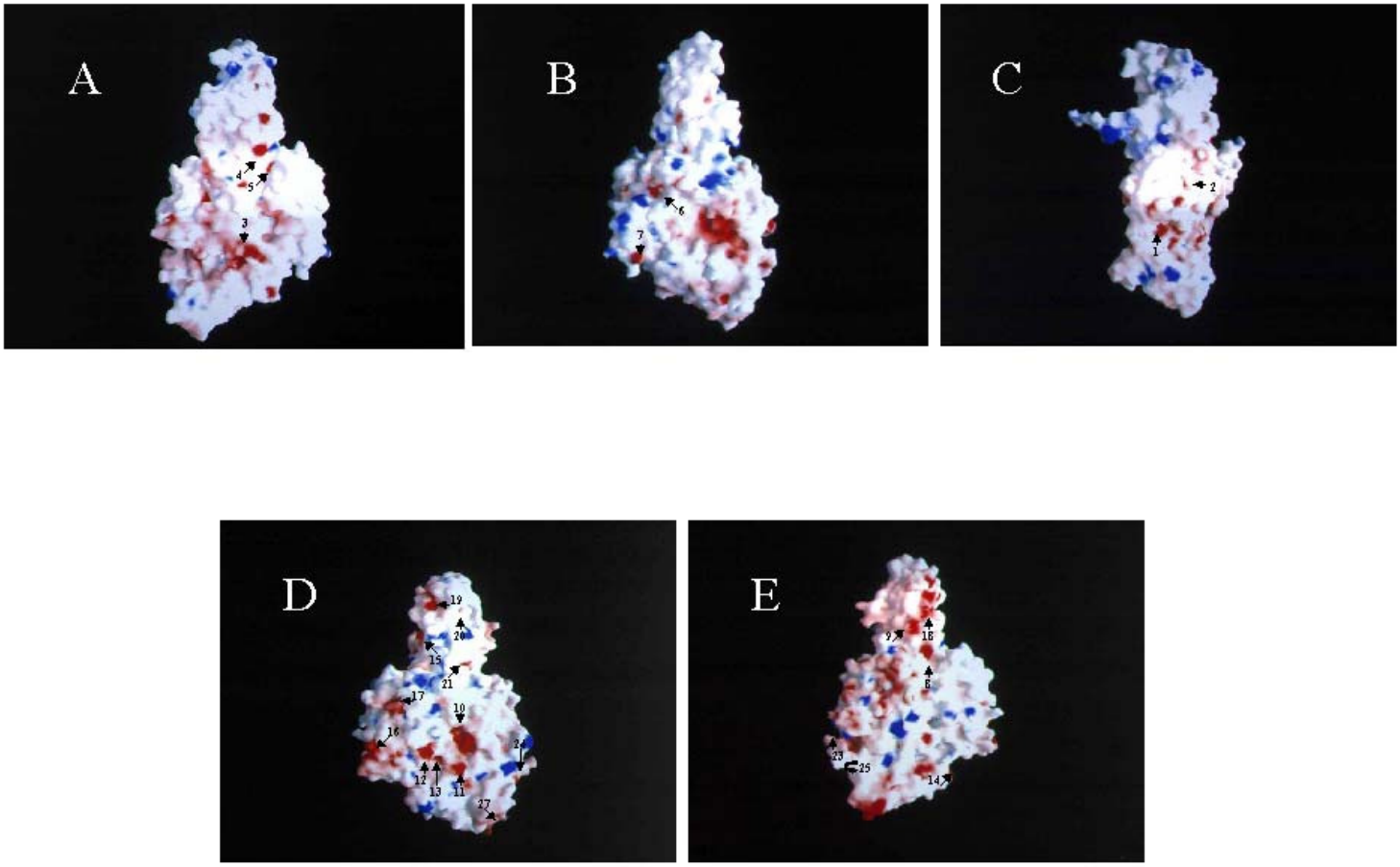

Figure 5. Electrostatic surface polarity analysis on FXIII-A and TGase 2. a-c show FXIII-A from three sides (on c, the recently determined Ca^{2+} binding site can be seen as 1; d and e show TGase 2 from two meaningful sides. Red areas mean higher local density of the negatively charged amino acids (potential Ca^{2+} binding sites; only the clusters with the highest negativity are numbered according to Table 1) while blue areas represent positive charges. As can be seen, the TGase 2 has more possibilities to bind Ca^{2+} than the FXIII-A.

Table 1.

Potential Ca^{2+} binding sites of FXIII-A and TGase 2 by surface polarity analysis

	Negatively charged amino acids with high surface potential[a]	Negatively charged amino acids with low surface potential[a]
FXIII-A	Asp438[1], Glu377[2], Asp219[3], Asp67[4], Glu231[5], Asp297[6], Glu658[7]	Glu489, Asp532, Glu203, Asp58, Asp357, Glu593, Glu495, Glu489
Human TGase 2	Asp25[8], Asp20[9], Asp306[10], Glu329[11], Asp242[12], Glu557[13], Glu549[14], Asp11[15], Glu637[16], Asp259[17], Glu15[18], Glu4[19], Glu120[20], Asp210[21], Asp87[22], Glu467[23], Glu469[24], Glu569[25], Asp581[26], Glu322[27]	Glu585, Glu539, Asp490, Glu535, Asp434, Glu8, Asp553, Asp389, Glu549

[a]We grouped the negatively charged amino acids exposed at the molecular surface (Figure 5) by an arbitrary manner into two groups shown above according to their surface potentials. Amino acids possessing greater than 30 relative units (GRASP-program) of potential were referred to as having "high surface potential" while those below 30 have "low surface potential". We designated here only one amino acid (with the highest potential) from a negatively charged pocket i.e. everyone represents one separate potential Ca^{2+} binding site. Clusters with higher surface potential should probably be considered first as potential Ca^{2+} binding sites, however, there could be local structural determinants that enhance Ca^{2+} affinity of sites having lower potential. Numbering is related to Figure 5.

In almost all Ca^{2+} binding proteins (except those which contain EF-hands) the Ca^{2+} binding sites are composed of amino acids which are considerably distant in the primary sequence such as in the case of the recently determined Ca^{2+} binding site of FXIII-A (Asp438, Ala457, Glu485, and Glu490). This supports the claim that any amino acid composition, which possesses negative surface potential, can be taken into account as a potential Ca^{2+} binding site. Thus, the potential Ca^{2+} binding sites of the two TGases can be determined on the basis of their potential surfaces. It has been suggested, based on primary sequences, that generally there are three consensus Ca^{2+} binding sites in the TGases [86]. For human TGase 2, the three putative Ca^{2+} binding sites are the following: 146-162, 229-234 and 434-452 [83]. The 146-162 and the 434-452 regions appear as highly negative clusters on the polarity-surface, while the 229-234 region has negligible negative surface-potential.

In the most Ca^{2+} dependent enzymes the binding of a limited number of metal ions are enough for the expression of the required conformational changes. Therefore, it is not necessary that all the Ca^{2+}s bound to TGases have a role in the activation processes especially because some of them are loaded only at higher Ca^{2+} concentrations (see below). These may be bound passively with respect to the activation processes probably possessing Ca^{2+} buffering roles. However, the structural explanation of the Ca^{2+} activation process of TGases is still missing and it cannot be ruled out that all or most of these

```
            51                                                  100                                                 150
tglc_human  FEGRNYQASV D..SLTFSVV TGPAPSQEAG TKARFPL... .RDAVEEGDW TATVVDQQDC TLSLQLTTPA NAPIGLYRLS ..LEASTGYQ GSSFVL....
f13a_human  FS.RPYDPRR DLFRVEYVI. .GRYPQENKG TYIPVPIVSE L....QSGKW GAKIVMREDR SVRLSIQSSP KCIVGKFRMY VAVWTPYGV. ...LRTSRNP
tgl3_human  M.NKGLGSN. E..RLEFIDT TGPYPSESAM TKAVFPL... .SNG.SSGGW SAVLQASNGN TLTISISSPA SAPIGRYTMA LQIFSQGG.. ISSVKL....

            151                                                 200                                                 250
tglc_human  .GHFILLFNA WCPADAVYLD SEEERQEYVL TQQGFIYQGS AKFIKNIPWN FGQFQDGILD ICLILLDVNP KFLKNAGRDC SRRSSPVYVG RVGSGMVNCN
f13a_human  ETDTYILFNP WCEDDAVYLD NEKEREEYVL NDIGVIFYGE VNDIKTRSWS YGQFEDGILD TCLYVMD... ...R.AQMDL SGRGNPIKVS RVGSAMVNAK
tgl3_human  .GTFILLFNP WLNVDSVFMG NHAEREEYVQ EDAGIIFVGS TNRIGMIGWN FGQFEEDILS ICLSILDRSL NFRRDAATDV ASRNDPKYVG RVLSAMINSN

            251                                                 300                                                 350
tglc_human  D.DQGVLLGR WDNNYGDGVS PMSWIGSVDI LRRWKNHGCQ RVKYGQCWVF AAVACTVLRC LGIPTRVVTN YNSAHDQNSN LLIEYFRNEF GEI..QGDKS
f13a_human  D.DEGVLVGS WDNIYAYGVP PSAWTGSVDI LLEYRSS.EN PVRYGQCWVF AGVFNTFLRC LGIPARIVTN YFSAHDNDAN LQMDIFLEED GNVNSKLT.K
tgl3_human  D.DNGVLAGN WSGTYTGGRD PRSWDGSVEI LKNWKKSGFS PVRYGQCWVF AGTLNTALRS LGIPSRVITN FNSAHDTDRN LSVDVYYDPM GNPLDKG..S

            351                                                 400                                                 450
tglc_human  EMIWNFHCWV ESWMTRPDLQ PG....YEGW QALDPTPQEK SEGTYCCGPV PVRAIKEGDL STKYDAPFVF AEVNADVVDW IQQD.DGSVH KSIN...RSL
f13a_human  DSVWNYHCWN EAWMTRPDLP VG....FGGW QAVDSTPQEN SDGMYRCGPA SVQAIKHGHV CFQFDAPFVF AEVNSDLIYI TAKKDGT..H VVENV..DAT
tgl3_human  DSVWNFHVWN EGWFVRSDLG PP....YGGW QVLDATPQER SQGVFQCGPA SVIGVREGDV QLNFDMPFIF AEVNADRITW LYDNTTGKQW KNSV...NSH

            451                                                 500                                                 550
tglc_human  IVGLKISTKS VGRDE..... .REDITHTYK YPEGSSEERE AFTRANHLNK LAEK..... .......EET GMAMRIRVGQ SMNMGSDFDV FAHITNNTAE
f13a_human  HIGKLIVTKQ IGGD...... GMMDITDTYK FQEGQEEERL ALETA..... ..LMYGAKKP LNTEGVMKSR SNVDMDFEVE NAVLGKDFKL SITFRNNSHN
tgl3_human  TIGRYISTKA VGSNA..... .RMDVTDKYK YPEGSDQERQ VFQKALGKLK PNTPFAATSS MGLETEEQEP SIIGKLKVAG MLAVGKEVNL VLLLKNLSRD

            551                                                 600                                                 650
tglc_human  E.YVCRLLLC ARTVSYNGIL GPECGTKYLL NLTLEPFSEK SVPLCIL.YE KYRDCLTESN LIKVRALLVE PVINSYLLAE RDLYLENPEI KIRILGEPKQ
f13a_human  R.YTITAYLS ANITFYTGVP KAEFK.KETF DVTLEPLSFK KEAVLIQ.AG EYMGQLLEQA SLHFFVTARI NETRDVLAKQ KSTVLTIPEI IIKVRGTQVV
tgl3_human  T.KTVTVNMT AWTIIYNGTL VHEV.WKDSA TMSLDPEEEA EHPIKIS.YA QYERYLKSDN MIRITAVCKV P.DESEVVVE RDIILDNPTL TLEVLNEARV

            651                                                 700
tglc_human  KRKLVAEVSL QNPLPVALEG CTFTVEGAGL TEEQKTVEIP DPVEAGEEVK
f13a_human  GSDMTVTVQF TNPLKETLRN VWVHLDGPGV TR.PMKKMFR .EIRPNSTVQ
tgl3_human  RKPVNVQMLF SNPLDEPVRD CVLMVEGSGL LLGNLKIDVP .TLGPKERSR
```

Figure 6. Multiple sequence alignment of TGases. Only the examined three TGases are shown, however originally 18 primary sequences were fit together (namely: 42_human, 42_mouse, annu_scham, f13a_human, tgl3_human, tgl3_mouse, tgl4_human, tglc_bovin, tglc_cavcu, tglc_chick, tglc_human, tglc_mouse, tglc_pagma, tgld_rat, tglh_tactr, tglk_human, tglk_rabit, tglk_rat). Single letter codes of the two amino acids with negatively charged side-chains are boldface (**D**, **E**) while the corresponding electron-donor amides are italicized (Q, N) in order to highlight the potential residues capable of having a role in Ca^{2+} binding. Yellow sequences contain a relatively higher number and density of negatively charged amino acids and could be assigned as potential Ca^{2+}-binding sites, but only according to the primary sequences. Sequences designated with red letters (originally yellow) are exposed at the surface according to surface polarity analysis. N- and C-termini containing no potential Ca^{2+}-binding sequences are not presented.

sites have a role in triggering and/or stabilizing of the catalytically active conformation in various *in vivo* settings.

TGase 3 has several negatively charged regions in its primary sequence and some of them are homologous to those of TGase 2 and FXIII-A; these can be predicted as potential Ca^{2+} binding sites.

7.1.2. Characterization of the enzymes studied by NMR

The purification of FXIII-A_2 and TGase 3 into their appropriate pure state was carried out using previously applied methods and their properties were found to be equivalent to those published [59, 60]. Human TGase 2 was purified as a GST-fusion (25.5kDa) and showed the same characteristics as determined elsewhere [88]. The FXIII-A_2 was treated with thrombin while TGase 3 with dispase. The purity of the enzymes and the performed cleavages could be followed on Coomassie-stained gels (Figure 7).

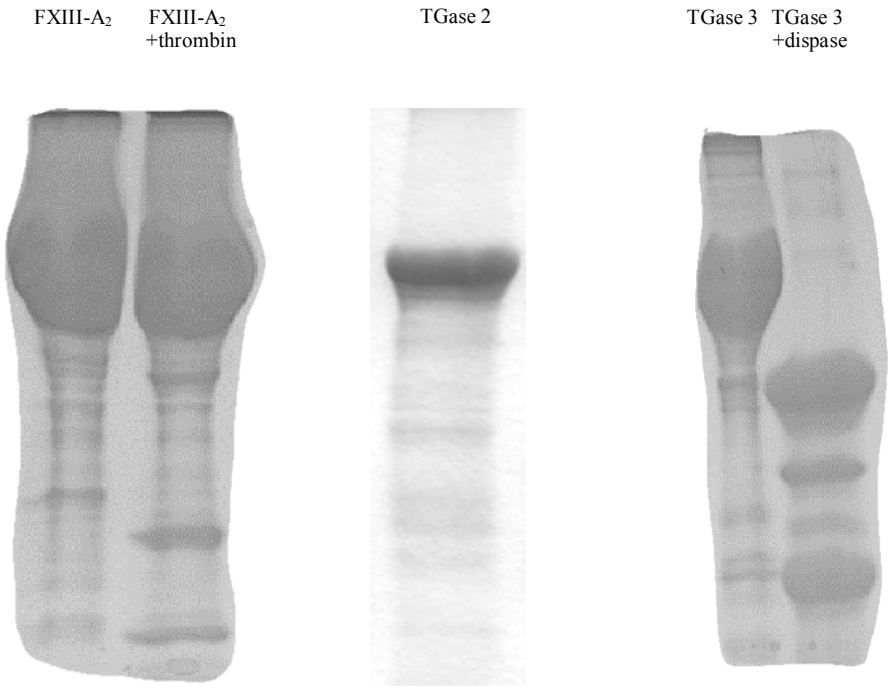

Figure 7. The SDS-PAGE of TGases. The gels are overloaded for checking the purity of the enzyme preparations which was always >90% by densitometry. Molecular weight standard is not pictured because of different gels and overload.

Catalytic efficiencies of the enzymes were tested by the amine-incorporation activity assay (Table 2). Each enzyme showed the expected activation pattern by Ca^{2+} and proteases (FXIII-A_2 and TGase 3) naturally with different specificity to the applied substrate. Thrombin could activate FXIII-A_2 very effectively. FXIII-A_2 was treated by 1M NaCl to achieve activation without thrombin; as expected, approximately 1.5-times higher specific activity was observed than by thrombin [10]. A decreased amount of activity was also found at nearly physiological concentration of salt and even without any salt possibly because of the presence of a small amount of proteolytically activated enzyme. GTP could totally inhibit the human TGase 2. Dispase treatment resulted in a significant increase in the activity of TGase 3.

7.1.3. Titration with $^{43}Ca^{2+}$

TGases were titrated with Ca^{2+} in the concentration range of 1mM – 51mM and the overall transverse relaxation rate of the Ca^{2+} nuclei was measured (Table 3). A typical ^{43}Ca NMR titration experiment is shown in Figure 8 while Figure 9 shows the evaluation process. The average dissociation constants of the Ca^{2+}-TGase complexes (K_d) and the values of T_{2B}/n could be calculated as detailed above (Table 2). The relaxation rate of Ca^{2+} bound to protein can be expressed by equation 4 that contains only χ and τ_c as unknown variables, the values of which depend on the nature of the protein. The correlation time is approximately the linear function of the molecular weight (if the shape of the molecule is not very different). This value is 200ns for FXIII-A_2B_2 and 50ns for FXIII-B [7], therefore the actual values for different TGases could be calculated considering similarities in shape (30% sequence identity is generally enough for considering a very similar shape). In this manner, the χ (which reflects the symmetry of the Ca^{2+} binding sites) can be obtained from T_{2B}/n.

7.1.4. FXIII-A_2

For FXIII-A_2, four conditions were examined and all the obtained dissociation constants were in the millimolar range. These values are equal in magnitude to but higher than the one determined previously by equilibrium dialysis and intrinsic fluorescence in shorter Ca^{2+} concentration ranges (0.51mM by NMR versus 0.1mM, see citation 5) confirming that low affinity binding sites exist and are loaded at higher Ca^{2+} concentrations in accordance with the results of the surface polarity analysis

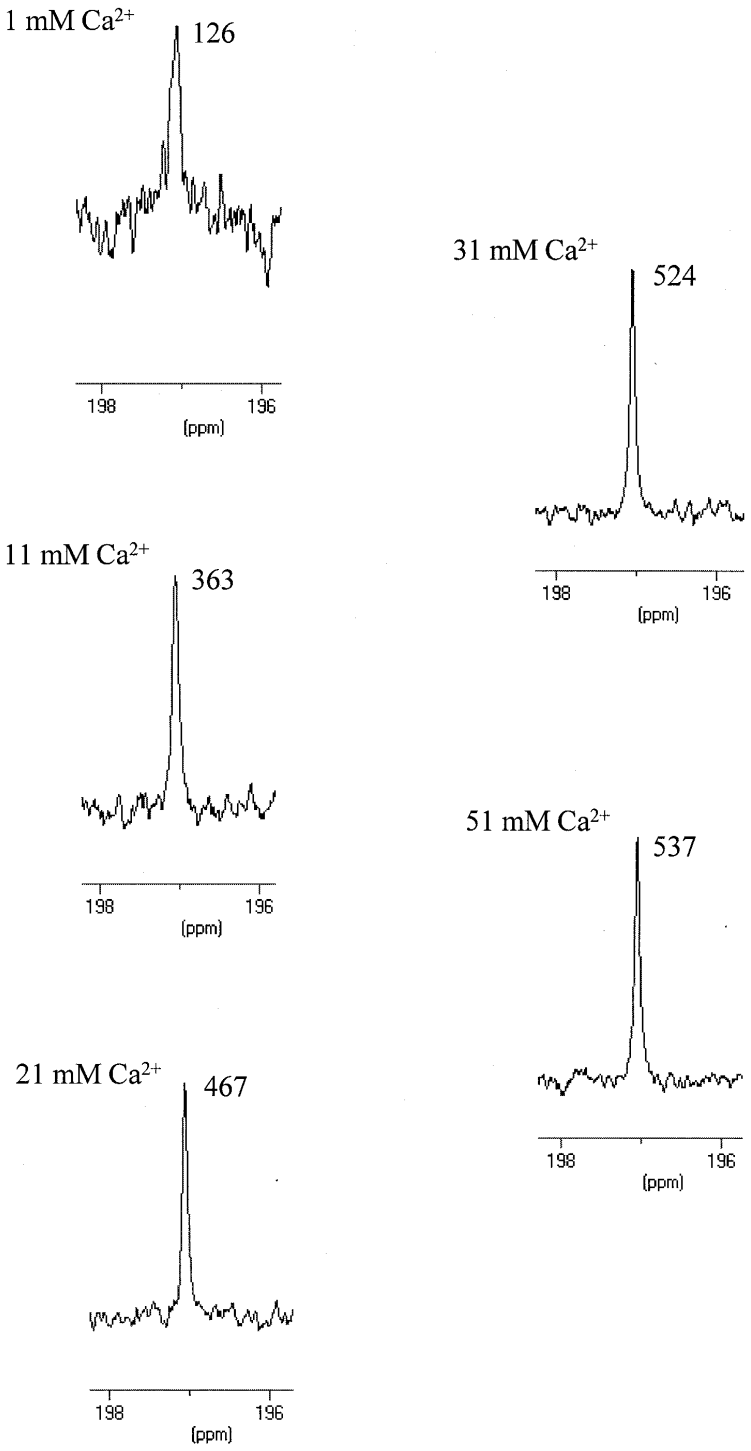

Figure 8. A ^{43}Ca NMR experiment. Lorentian ^{43}Ca signals and their peak-heights (in relative units) are shown at different Ca^{2+} concentrations in the presence of FXIII-A_2 (2.5µM protein, 50mM Tris, pH7.5). All signals measured after 14ms of relaxation showing clearly the decreasing relaxation rate upon increasing Ca^{2+} concentration.

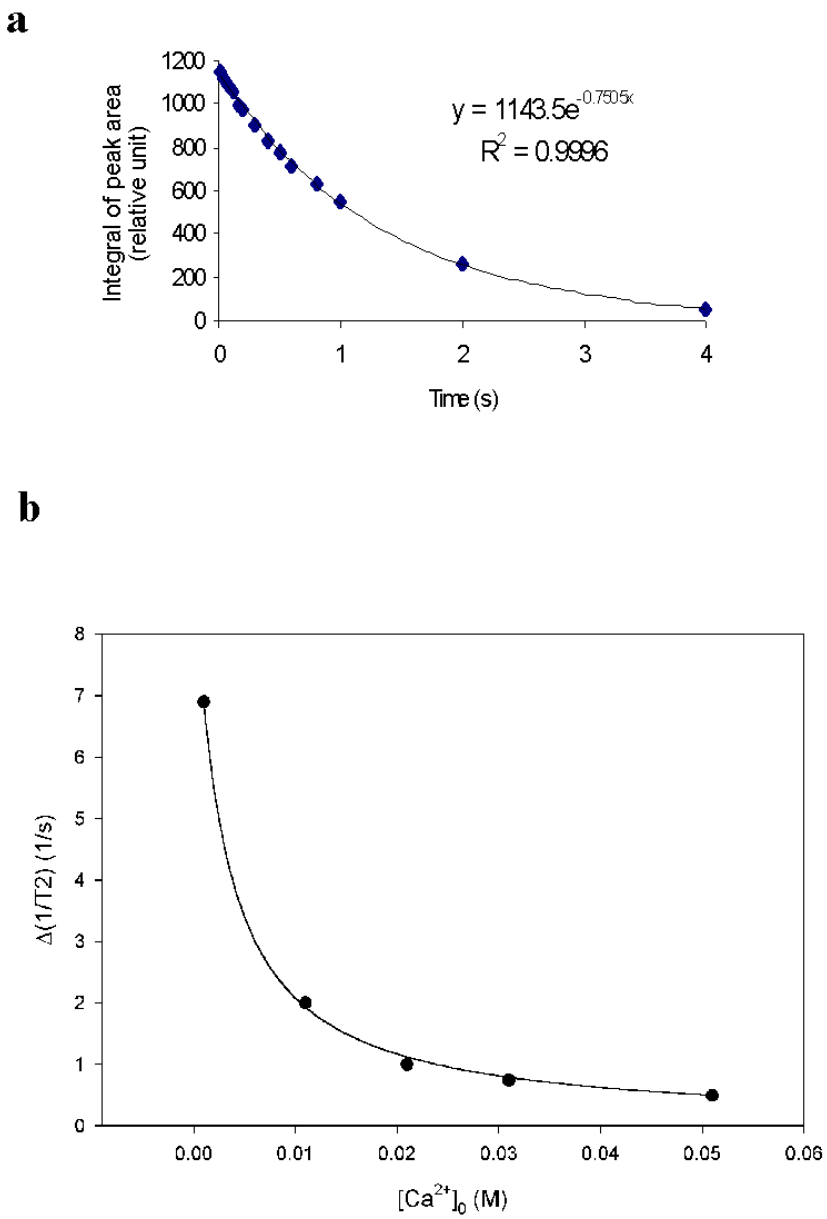

Figure 9. Evaluation of NMR results. a, A typical relaxation pattern of the ^{43}Ca nuclei according to a single exponential curve; b, The reduced relaxation rates are plotted versus the Ca^{2+} concentration fitting well to a hyperbolic function (Sigmaplot).

Table 2.

Applied enzyme concentrations in the NMR samples, specific activities, dissociation constants for Ca^{2+}-TGase complexes and the corresponding T_{2B}/n values[a]

Enzyme	[E] (μM)	Specific Activity (OD/min/mg)	$K_d \times 10^{-3}$ (M)	$T_{2B}/n \times 10^{-5}$ (s)
FXIII-A_2 (50mM Tris, pH7.5)	2.5	22.4	0.51	8.2
FXIII-A_2 (150mM NaCl, 10mM Tris, pH7.5)	2.2	26.4	2.9	8.2
FXIII-A_2 (1M NaCl, 50mM Tris, pH7.5)	2.5	156	4.7	12
FXIII-A_2 + Thrombin (50mM Tris, pH7.5)	2.5	110	5.9	8.5
TGase 2 (150mM NaCl, 10mM Tris, pH7.5)	2.9	2.20	6.0	2.8
TGase+GTP (150mM NaCl, 10mM Tris, pH7.5)	1.6	0.00	*$8x10^{6}$*	*$1.2x10^{11}$*
TGase 3 (150mM NaCl, 10mM Tris, pH7.5)	1.9	30.0	1.8	75
TGase 3+Dispase (150mM NaCl, 10mM Tris, pH7.5)	1.8	37.6	2.0	280
Thrombin (50mM Tris, pH7.5)	0.57	-	1.6	0.42

[a]The data are means of at least three measurements and have less than 5% error.

. **Table 3.**

Reduced relaxation rates of Ca^{2+} nuclei in the absence and presence of different TGases[a]

	Reduced Relaxation Rates (1/s)									
$[Ca^{2+}]$ (mM)	FXIII-A_2 +No salt Buffer B	FXIII-A_2 +150mM salt Buffer A	FXIII-A_2 [b] +1M salt Buffer B	FXIII-A_2 [b] +thrombin Buffer B	TGase 2 Buffer A	TGase 2 + GTP Buffer A	TGase 3 Buffer A	TGase 3 +dispase Buffer A	Thrombin[b] Buffer B	No enzyme Buffer A
1	20	6.9	3.0	-	15	-	0.90	0.21	38	0.96
11	2.8	2.0	1.4	4.2	6.5	-	0.17	0.047	11	0.84
21	1.1	1.0	0.73	1.2	3.8	32	0.15	0.028	5.6	0.83
31	0.98	0.74	0.83	0.66	2.8	17	0.080	0.024	4.4	0.75
51	0.57	0.49	0.63	0.63	-	7.7	-	-	3.0	0.68

[a]The data, which could not be determined precisely, were neglected from fitting and from this table (in some cases at very high concentrations of Ca^{2+}, the values of the reduced relaxation rates contained relatively big uncertainties, while at very small concentrations sometimes this rate was too large to determine precisely). The data are means of at least three measurements and have less than 5% error. [b] First point measured at 2mM Ca^{2+} instead of 1mM for experimental reasons. Buffer A: 150mM NaCl, 10mM Tris, pH7.5; Buffer B: 50mM Tris, pH7.5.

and as predicted earlier [9]. If we calculate the binding of only one Ca^{2+}/subunit FXIII-A (that is two for the whole molecule, n=2 and represents low Ca^{2+} concentrations) [8] and 100ns of correlation time, we get 0.37MHz for the average of χ. In an EF-hand like Ca^{2+} binding motif χ would be ~ 1MHz. This confirms previous results that the main Ca^{2+} binding site of FXIII is not an EF-hand like motif and shows that Ca^{2+} is not in a tight environment (the amino acids probably are at farther distances from Ca^{2+}) as determined earlier in the crystalline phase [8].

X-ray studies showed that in FXIII-A there is only one direct ligand toward Ca^{2+}, which is the Ala457-O; all the other direct ligands are water molecules. The previously published ligands (Asp438, Ala457, Glu485 and Glu490) are not close enough to be real Ca^{2+} ligands (Sicker, Weiss and Hilgenfeld, unpublished results). Interestingly, on the polarity surface of FXIII-A, the Glu485 and the Glu490 do not possess considerable negative potentials, only Asp438 and its proximal area show dense negativity. The more Ca^{2+} binding sites we suppose, the less the average χ is, so it is impossible to get into the range of 1MHz (if n=8, χ=0.19). It is not probable that there are binding site(s) with big differences in symmetry (to satisfy these small average values of χ) [9, 18] so it seems that the whole protein molecule lacks EF-hands as sequence analysis suggests [5].

We found that upon increasing the concentration of inert salt, the K_d increased. That is the Ca^{2+} affinity decreased, as suggested elsewhere [10]. The thrombin-cleavage decreased the Ca^{2+} affinity of the enzyme in contrast with earlier data showing no considerable effects [9]. It is interesting that the thrombin-activation and the salt-effect (at low concentration) decreased the Ca^{2+} affinity but it did not significantly change the average symmetry of the binding sites (as the negligible changes of T_{2B}/n show, since n can be considered constant; see Table 2). One interpretation of these results is that those amino acids which move during activation do not cause great overall conformational change in the binding sites but rather induce a significant decrease in the level of attractive forces probably by increasing the distance between the donor groups and Ca^{2+}. In 1M NaCl, both the affinity and the χ decreased (0.31MHz, if n=2) suggesting another basis for the two activation processes. So far, there are two considerable explanations for the mechanism of the Ca^{2+} induced activation processes of TGases. According to the first suggestion, the switch to the catalytically active conformation is triggered by the isomerization of the non-proline cis-peptide bonds (which are well-conserved in the TGase family) to trans conformations promoting the separation of domain 2 and 3 exposing the active site [6]. Upon the second proposal, the separation of the same two domains is forced by a direct Ca^{2+} effect by which the loop between the two domains is distorted making the active site accessible [83]. Since the activation of cellular FXIII by 1M NaCl does not need any proteolytic cleavage, probably it undergoes on the second pathway. We also determined the K_d of the Ca^{2+}-thrombin complex and found it to be in the millimolar range (Table 2).

We performed ^{25}Mg NMR experiments on FXIII-A_2 to confirm earlier studies stating that Mg^{2+} does not bind to the protein [9]. There was no considerable change in the relaxation rate when protein was added to $^{25}Mg^{2+}$ (Figure 10) even at higher Mg^{2+} concentrations. A possible reason for this resistance could be related to the preferred formation of inner-sphere over outer-sphere complexes and subsequently to the higher spatial requirements of the hydrated Mg^{2+}.

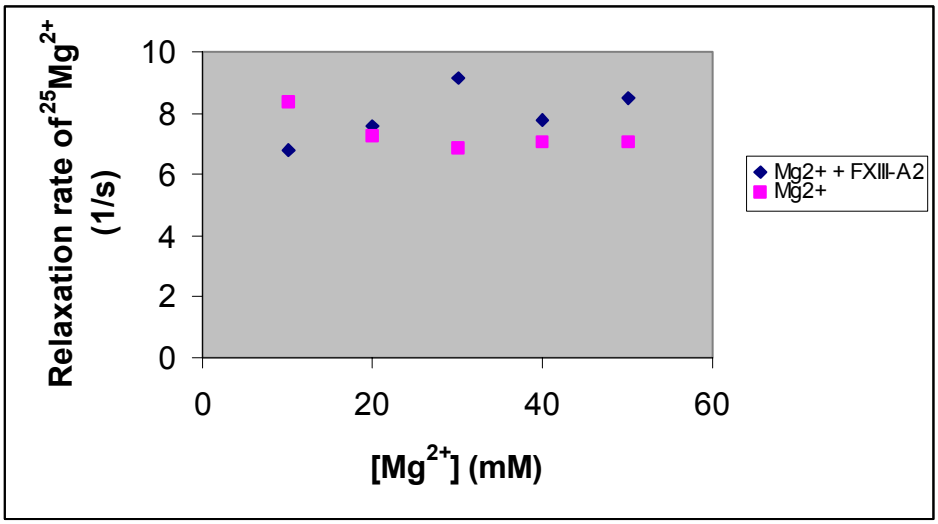

Figure 10. The transverse relaxation rate of $^{25}Mg^{2+}$ versus Mg^{2+} concentration in the absence and presence of FXIII-A_2. There is no considerable difference suggesting that Mg^{2+} does not bind to FXIII.

7.1.5. TGase 2

The enzyme was expressed as a GST-fusion for easier purification. It has been reported that it is not necessary to cleave the GST-fusion during investigations of the enzyme [88], especially because GST does not bind Ca^{2+}. The TGase 2 showed millimolar affinity to Ca^{2+}; the value of K_d practically equals that of the thrombin-activated FXIII-A_2 suggesting analogous activation processes and similar active conformations for the two TGases. This average K_d value is higher than the one determined previously (6.0mM by NMR versus 0.09mM, see citation 18). Since we made measurements on a wider concentration scale than that used in the previous equilibrium dialysis experiment, our study verifies the existence of low affinity Ca^{2+} binding sites on the TGase 2 molecule (similarly to FXIII-A_2) loaded only at higher Ca^{2+} concentrations as suggested by our surface polarity analysis and by earlier indirect experiments [19].

Evaluation provided χ=0.48MHz for the enzyme calculated with six Ca^{2+} binding sites (low Ca^{2+} concentrations)[18] and τ_c=60ns (due to the GST-fusion; from linear extrapolation, see above) which suggests that this TGase does not have EF-hand motifs, either. According to the average symmetry parameters, the Ca^{2+} binding sites of TGase 2 are more asymmetric than those of FXIII-A_2 calculating only the number of high affinity binding sites loading at low Ca^{2+} concentrations. Taking into consideration more bound Ca^{2+}s the same trend remains. An explanation can be that in TGase 2 the bound Ca^{2+}s are more buried by amino acids or the donor groups are closer. However, it seems that it does not interfere with the approximately same values of K_ds.

Human TGase 2 behaved as expected in the presence of GTP since practically zero binding efficiency to Ca^{2+} was observed when GTP was present. The high values of K_d and T_{2B}/n show that not only the strength of the binding but the number of the binding sites also decreased practically to zero: because T_{2B} cannot be such a high value, only the very small value of n could cause this effect. It shows that the binding of GTP to the enzyme eliminates all the Ca^{2+} binding sites including the low affinity ones; the structural explanation of this phenomenon is the target of further speculations. It confirms previous proposals that there is a conformational switch after the binding of GTP to TGase 2 and not only a chelation effect takes place [18]. The fact that in the presence of 51mM Ca^{2+} and 10mM GTP there was not any observable Ca^{2+} binding left strengthens the finding that the GTP-TGase 2 complex is much tighter than the Ca^{2+}-TGase 2 complex [89].

7.1.6. TGase 3

Human TGase 3 has special properties including shape and activation [25] which are distinguishing this enzyme from the above mentioned two TGases. There have been no suggestions for the number, localization and affinities of its Ca^{2+} binding sites. The obtained K_d represents that TGase 3 exceeds the other two TGases in almost all conditions in Ca^{2+} affinity (except the unactivated FXIII-A_2). After proteolytic activation, TGase 3 partially lost its affinity to Ca^{2+}, as did FXIII-A_2. Correlation time of 60ns was calculated for the molecule before proteolysis (this protein has a more elongated shape [25] than the other two TGases; 30% increase in correlation time was calculated and applied). After the cleavage, for the 50kDa and the 27kDa parts 30 and 15ns were calculated, respectively (shrunk shape). Considering the same total number of binding sites before and after proteolysis, χ is smaller after the activation of TGase 3 (if n=1, χ=0.23 and 0.14MHz, respectively) which is in good agreement with the decreasing affinity (Ca^{2+} may stand at outer regions of the protein). If we increase n, both χs decrease remarkably (according to equation 4).

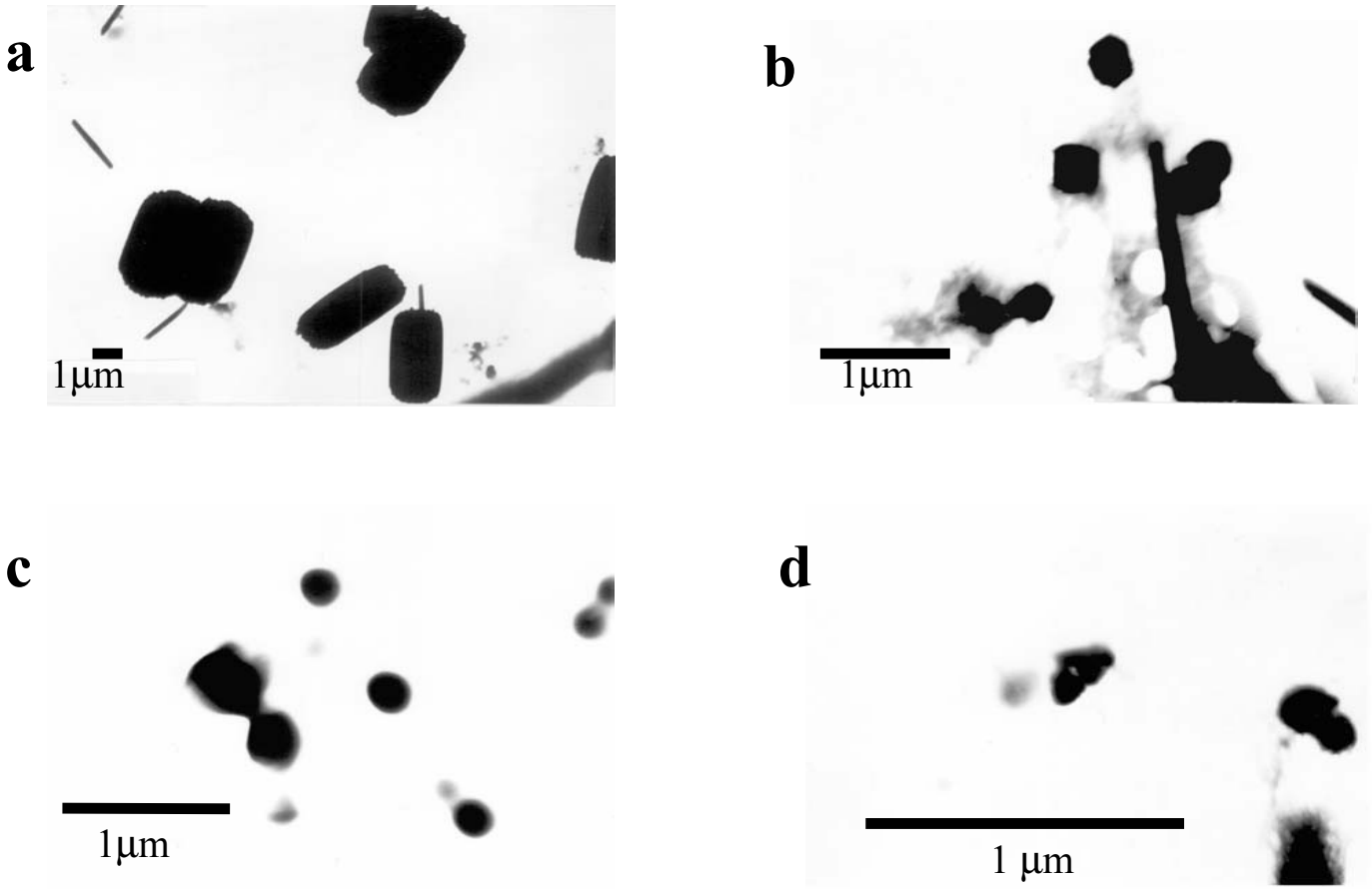

Figure 11. Electronmicroscopic representation of the inclusion bodies in the four main processing steps. a., E.coli bacteria in the culture b., Sonicated culture with appearing inclusion bodies and cell debris c., Inclusion bodies after washing with 2M urea d., Inclusion bodies in their reduced sizes after the 8M urea treatment.

7.2. Refolding studies on TGase 2

7.2.1. Results

In the starting phase of our experiments expression and analysis of the recombinant human tissue transglutaminase in *E.coli* was carried out as described. It was concluded from activity measurements and Western blot results that inclusion bodies were present in the system because the TGase 2 was detected in varying concentrations in each fraction during the processing steps and there was a fraction which could only be unfolded by 8 M urea (data not shown).

Main steps were followed by electronmicroscopy to verify the presence of inclusion bodies according to their size and geometry (Figure 11) [52]. At this stage, the yield of inclusion body production was optimized by changing the parameters of the bacterial expression and processing (see Materials and Methods section). We could get 0.65g of inclusion body and 125µg of unfolded TGase 2 (maximum extracted mass of TGase from the inclusion bodies) from one liter of bacterial culture. Obtaining 21.2 % recovery for total mass of protein could be extracted from inclusion bodies, the percentage of TGase 2 in the inclusion bodies calculated to be ~ 0.1% which is similar to cases of such large proteins studied [52]. The SDS-PAGE and ECL-Western blot analysis of inclusion body proteins confirmed the unambiguous presence but this limited percentage ratio of the enzyme (Figure 12).

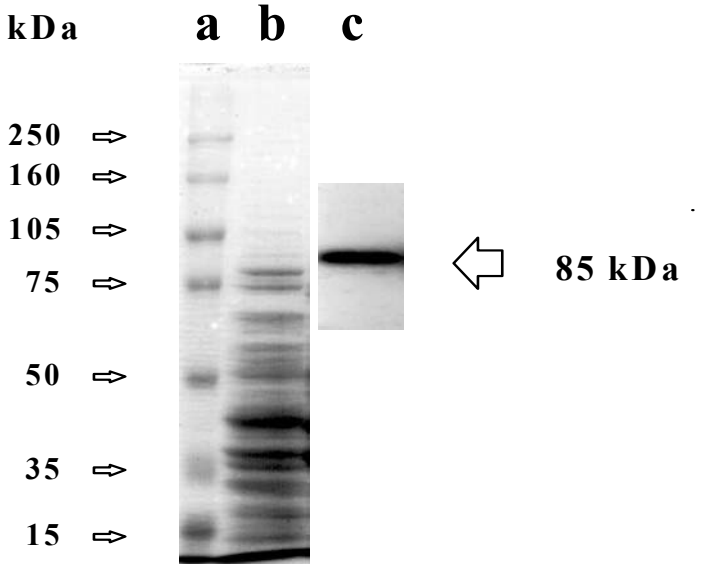

Figure 12. Analysis of the inclusion bodies by SDS-PAGE and ECL-Western blot. Lane a: MW standard; lane b: 2M urea-washed inclusion bodies using SDS-PAGE and Coomassie B-Blue staining; lane c: 2M urea-washed inclusion bodies, Western blot using monoclonal antibody against TGase 2.

For washing the inclusion bodies, only 2M urea was applied since the elimination of Triton X-100 from the refolding mixtures showed difficulties. Another redox-shuffling agents than cysteine/cystine (such as glutathione), another pH and molecular mass of PEG were not applied because of the proposals of the mentioned references [52, 90].

For refolding, firstly we used a buffer (1mM EDTA, 1mM cysteine, 0.1mM cystine, pH10.0) containing varying chemicals to help the process (see Material and Methods section) since the successive elimination of the denaturant (even in the presence of Ca^{2+} and GTP) seemed to be inefficient. Figure 13 represents the effects of the helper materials. As can be seen, the 5% PEG was the most efficient refolding agent. When PEG was dialyzed out using the solution of 1mM EDTA, 1mM cysteine, 0.1mM cystine, 0.1M Tris, pH8.5, an 83% increase could be observed in the enzyme activity. The enzyme activity could also be measured by a specific radioactive substrate incorporation assay and it could be inhibited by iodo-acetamide (TGases have a cysteine in their active sites) and by Mg-GTP (data not shown) [79].

Considering the amount of the unfolded TGase 2, regained activity and dilution factors, the activity/weight ratio of the recombinant enzyme was 21.84 OD/min/mg (if we consider only the mass of the extracted TGase 2; evaluating with the total protein content, the real specific activity is naturally much less). This is comparable in magnitude to the specific activity of the Guinea pig enzyme (42.5 OD/min/mg)

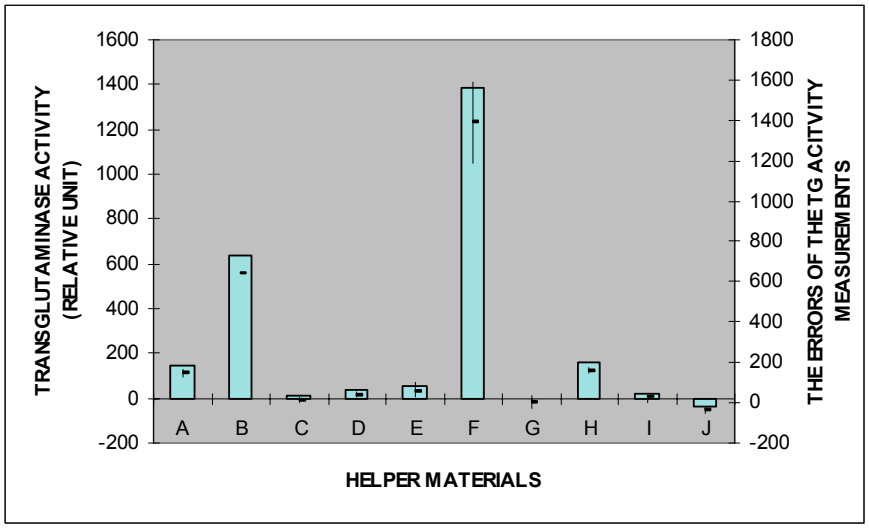

Figure 13. Effects of different helper materials to the refolding process of recombinant human TGase 2. A: 1mg/ml bovine serum albumine (BSA); B: 5% PEG; C: 0.1% Triton X-100; D: 10% glycerol; E: Control (sample handled in the same way but without any helper material); F: Guinea pig liver transglutaminase, 5µg/ml, positive control in the activity measurement; G: 1M Tris; H: 10mg/ml lauryl maltoside; I: 33mM CHAPS; J: 0.5M arginine hydrochloride.

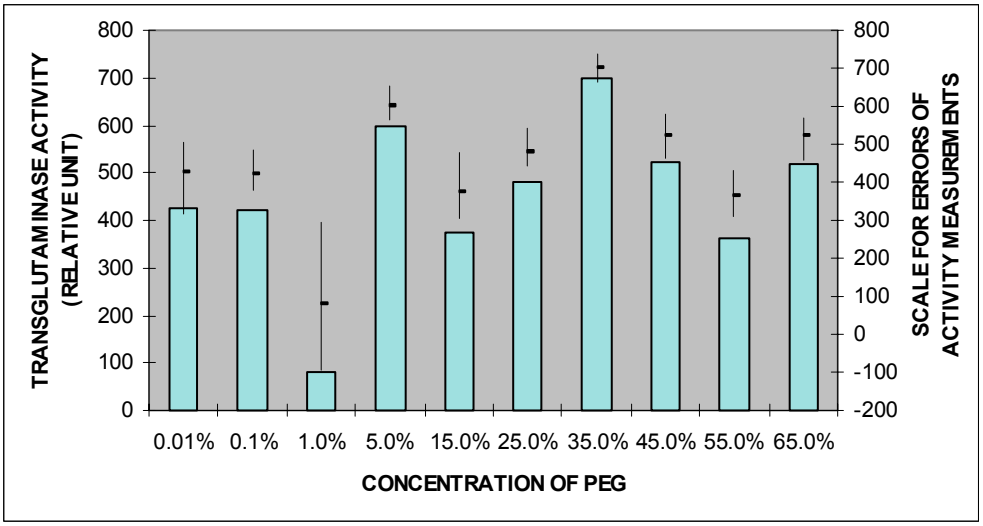

Figure 14. Activity of the refolded recombinant human TGase 2 as a function of PEG concentration. The most effective concentrations are the 5% and 35%.

prepared from liver (Sigma) verifying the successful reconstruction of the protein structure.

Since PEG overtook the other agents in restoring TGase activity, its concentration dependence was studied next (Figure 14). The most effective refolding concentrations of PEG were the 5m/w% and 35m/w%. The removal of PEG in the case of 35% PEG caused almost the same increase in activity (80%).

The structural features of TGase 2 suggest that Ca^{2+} and Mg-GTP/Mg-ATP may affect its folding. Therefore, we examined the effects of Ca^{2+} and GTP/ATP on the folding process in 5 and 35 % PEG. Experiments were performed as described using EDTA, Ca^{2+}, GTP and ATP in all combinations in the folding buffers constructing a widespread analysis of the refolding behavior. Since in every case the dialysis of PEG out from the refolding mixtures resulted in higher activities only these experiments are discussed (Table 4). All the processes were followed in time. In almost all samples, activity maxima were found at around the third day after the second dialysis that removes PEG. After these activity maxima, there were samples showing continuous decrease or minimums and afterwards another maxima in activity. Results clearly show that Ca^{2+} and GTP/ATP also have a role in helping the folding of TGase 2 in both concentrations of PEG. Generally, Ca^{2+} was more efficacious on refolding than GTP/ATP, while GTP and ATP were equally efficient. However, the most effective condition (according to the final activities) was when Ca^{2+} and GTP were used together in 5% PEG and are removed along with PEG by the second dialysis buffer containing EDTA. Final TGase activities were reached generally after 20 days and were stable for one week at 4 ^{0}C.

Table 4.

TGase activity as a function of refolding conditions and time (after second dialysis)

	EDTA			Ca^{2+}			GTP			ATP			PEG	INHIBITORY			TGase activity[a] DAY			
	I	II	III	I	II	III	I	II	III	I	II	III	5%	35%	GTP	ATP	1	3	5	22
1	+	+	+										+				41	46	13	31
2	+	+	+										+		+		51	44	28	13
3	+	+	+										+			+	62	36	21	23
4				+	+	+							+				23	49	23	54
5				+	+	+								+			41	90	62	77
6							+	+					+				31	51	44	33
7							+	+						+			18	36	15	26
8										+	+		+				18	49	28	33
9										+	+			+			23	51	31	26
10			+	+	+		+	+					+				**21**	**90**	**69**	**100**
11				+	+	+	+	+					+				28	62	44	26
12			+	+	+		+	+						+			8	31	10	13
13				+	+	+	+	+						+			21	87	33	54
14			+	+	+					+	+		+				13	77	51	38
15				+	+	+				+	+		+				36	56	28	38
16			+	+	+					+	+			+			21	46	18	21
17				+	+	+				+	+			+			33	69	41	36

[a]Data are given in the percentage of the highest value. The most effective condition was when Ca^{2+} and GTP were applied together in 5% PEG. I: dilution buffer, II: dialysis buffer I, III: dialysis buffer II.

7.2.2. Conclusions of refolding results

Recombinant human tissue transglutaminase was successfully cloned and expressed from *E.coli*. Most of the recombinant enzyme was found in inclusion bodies from which the TGase 2 was successfully refolded under different experimental conditions. The experiments have led to several

interesting results related to the folding of human TGase 2. Since there were protein impurities in the refolding samples, only the recovery of the enzyme activity could be followed. Nevertheless, the effects of various affectors could be unambiguously explained by measuring the recovery of enzyme activity.

The results clearly show that PEG was the most efficient agent in facilitating the folding process. One of the striking observations of our study is the existence of two optimal concentrations of PEG for the refolding of TGase 2. Interestingly, the factor XIII zymogen also undergoes a phase transition in the crystalline state when the PEG concentration (which was used as precipitant) was increased up to about 34-36(w/v)% [90]. The increase of the PEG concentration led not only to a reordering of the factor XIII dimers in the crystal lattice, but also to a slight reorientation of the four domains relative to one another. This confirms our observation that PEG has a special effect on the structure of TGases. In the case of our refolding experiments, a structural switch to a new folding pattern may happen during the initiation of refolding resulting in another active conformation.

The removal of PEG led to an increase in the final TGase activity, probably because of ceasing the structural hindrance effects which can take place on the already (probably just partially) refolded molecules and allowing them to proceed on a more favorable refolding pathway. Above results also show that the refolding needs PEG only in its initiation phase. Its helper effects (in the starting phase of refolding) is probably based on the allosteric influence of the huge number of polar hydroxyl groups in spatial vicinity on the long chain of PEG burying and orienting the protein chains towards each other in a space with smaller amounts of degree of freedom (some kind of "cage-effect"). It is very probable that the loss of these kinds of effects caused the ineffectiveness of helper molecules with smaller size.

The two main affectors (Ca^{2+} and GTP) of TGase 2 have enhancing effects on refolding confirming the general consideration that the ligands of a protein can allosterically help the folding of the protein molecule after its expression. It is a structurally significant result that Ca^{2+} and GTP are more efficient together. This may support our starting hypothesis that they help some molecular parts to be folded (particularly in the early phase of refolding helping the effect of PEG) strengthening allosterically each other in contrast to their opposite effects on the folded structure [79]. It seems that after the removal of PEG, Ca^{2+} and GTP from the solution, the rest of the molecule can refold better to complete the final structure. It confirms their real role only in the initiation phase of the refolding process and presumes their disadvantageous effects for the remaining refolding steps. However, Ca^{2+} and GTP did not have any positive influence on refolding in absence of PEG indicating the demand of a large macromolecule for the initiation of the refolding. This observation suggests that an action of macromolecule with effects similar to PEG is needed for launching the refolding of the human TGase 2 physiologically as well. Seeking the appropriate natural chaperon with analogue effects is the target of

further studies. In addition, the nature of the two optimal PEG concentrations, the changing of activity on the extended time scale observed and the effects of other possible affectors in comparison to the native situation is also the objectives of our further investigations. All the observations we made could support fundamental parameters for the molecular simulation of the refolding process of the enzyme. Since the optimized refolding procedure yields active recombinant enzyme, after the development of a productive purification procedure (considering the already published purification methods for the enzyme) our refolding system is an alternative source of the non-fused recombinant enzyme.

Since tissue transglutaminase plays a critical role in a number of intra- and extracellular processes probably, it is regulated not only at the level of expression but at the level of folding. Understanding of the refolding may provide ways to influence the action of this enzyme not only at the level of gene expression but also at the folding steps, which would lead us to another level of pharmacological regulation.

8. SUMMARY

The structural basis of the Ca^{2+} effect on transglutaminases is poorly defined. Therefore, it was our intention to initiate ^{43}Ca NMR, surface polarity analysis combined with multiple sequence alignment studies to obtain structural information about the Ca^{2+} binding properties of the Factor XIII-A_2, TGase 2 and TGase 3 (each of human origin). Since Ca^{2+} is also implicated in the folding of TGase 2, refolding studies were also performed to elucidate the nature of these effects.

1. We have constructed a new homology model of human TGase 2 on the basis of the highest resolution (2.1Å) X-ray structure of cellular FXIII zymogen available. Our structure is more accurate than all the previously published homology models of human TGase 2.
2. We have performed surface polarity analysis on the high resolution structure of cellular FXIII zymogen and on our homology model of TGase 2. Results are combined with that of the multiple sequence alignment of TGases and in this manner we could identify probably all the potential Ca^{2+} binding sites on these molecules; their numbers are more than reported earlier. From the previously published three putative sites of TGase 2, two possess negativity on the surface but the third one does not. Interestingly, in the recently determined high affinity binding pocket of FXIII, only one amino acid shows considerable negative potential on the molecular surface. The potential Ca^{2+} binding sites of all TGases can be predicted using the results of this analysis.
3. In accordance with the high number of negatively charged clusters in our surface polarity analysis, ^{43}Ca NMR provided higher (but still millimolar) average dissociation constants titrating on a wide Ca^{2+} concentration scale than previous studies did by equilibrium dialysis in shorter ranges. These results suggest the existence of low affinity Ca^{2+} binding sites on both FXIII-A and TGase 2 in addition to the well-known high affinity ones.
4. Increasing the salt concentration or activating with thrombin, FXIII-A_2 partially lost its original Ca^{2+} affinity in contrast to previous results, which showed no effects.
5. The NMR data suggests different mechanisms for the proteolytic and salt activation processes of FXIII.
6. The NMR provided structural evidence for the GTP induced conformational changes of TGase 2 molecule diminishing all of its Ca^{2+} binding sites.
7. The NMR data on the Ca^{2+} binding properties of the first analyzed TGase 3 are presented here; TGase 3 binds Ca^{2+} the most tightly which weakens after proteolytic activation.

8. The investigated TGases have very symmetric Ca^{2+} binding sites and no EF-hand motifs.
9. The refolding of the recombinant TGase 2 molecule to its catalytically active form from inclusion bodies essentially needs the presence of a helper material with higher molecular mass, but only in the initiation phase. In natural conditions it is probably a chaperon, while *in vitro,* it could be e.g. PEG.
10. Ca^{2+} and nucleotides are ascribed as effector molecules in the early phase of the structural reconstitution of TGase 2; the most efficient condition if they are together in the refolding buffer.
11. Two optimal concentrations of PEG (probably two different folding pathways) and a relatively long time scale (with two activity maxima) for the evolution of the final structure of TGase 2 were identified during its refolding.
12. An optimized refolding procedure of the non-fused recombinant TGase 2 is reported.

9. APPENDIX 1.

First we must define the "concentration of binding sites", [B]:

$$[B]=n[E]$$

$$(\text{and } [B]_0=n[E]_0)$$

The dynamic equilibrium is as follows:

$$B + M \rightleftharpoons BM$$

$$K_d=\frac{[B][M]}{[BM]} \longrightarrow [BM]=\frac{[B][M]}{K_d}$$

Since $[M] \cong [M]_0$

$$\frac{[BM]}{[M]_0}=\frac{[B]}{K_d}(=p_B)$$

$$[B]_0=[B]+[BM]$$

$$n[E]_0=[B]+\frac{[B][M]_0}{K_d} \longrightarrow n[E]_0=[B]\left(1+\frac{[M]_0}{K_d}\right)$$

$$[B]=\frac{n[E]_0}{1+\frac{[M]_0}{K_d}}$$

Since $p_B = \frac{[B]}{K_d}$

$$p_B = \frac{[B]}{K_d} = \frac{n[E]_0}{\frac{K_d + [M]_0}{K_d} K_d} = \frac{n[E]_0}{K_d + [M]_0} \qquad \textit{(Equation 2)}$$

This relation can be inserted into the equation 1 providing equation 3.

10. APPENDIX 2.

Since in the presence of 10mM GTP the relation below is no longer valid, the related equations must be different, as well.

$$[M] \cong [M]_0$$

In this condition:

$$[M] \cong [M]_0 - 0.01$$

That is why:

$$\frac{[BM]}{[M]_0} = \frac{[B]}{K_d} \left(= p_B\right) \qquad [B] = \frac{n[E]_0}{1 + \frac{[M]_0}{K_d}}$$

The valid formulas are:

$$\frac{[BM]}{[M]_0} = \frac{[B][M]}{K_d[M]_0} \left(= p_B\right) \qquad [B] = \frac{n[E]_0}{1 + \frac{[M]}{K_d}}$$

Combining the two equations:

$$p_B = \frac{[BM]}{[M]_0} = \frac{n[E]_0[M]}{[M]_0\left(K_d + [M]\right)} = \frac{n[E]_0\left([M]_0 - 0.01\right)}{[M]_0\left(K_d + [M]_0 - 0.01\right)}$$

Taking into consideration that the equation 1 must be supplemented by another part that is the Ca^{2+} bound to GTP:

$$R_{2obs} = \pi v_{1/2} = p_F R_{2F} + p_B R_{2B} + p_{GTP} R_{2GTP}$$

After the appropriate substitutions, the final formula (equation 6) is evident.

11. ACKNOWLEDGEMENTS

I am thankful to my supervisor **Prof. Dr. László Fésüs** – the Head of the Institute – that I could work in his research group and that he has sustained my progress. Many thanks to **Dr. István Bányai** (University of Debrecen, Department of Physical Chemistry) for teaching NMR and adjusting the ^{25}Mg and ^{43}Ca NMR experiments. I thank the theoretical and technical help in NMR to **Dr. Gyula Batta** (University of Debrecen, Research Group for Antibiotics) and **Dr. Katalin Kövér** (University of Debrecen, Department of Inorganic Chemistry), the recombinant cellular FXIII, TGase 3 and TGase 2 to **Dr. Hubert Metzner** (Centeon Pharma GmbH, Marburg, Germany) and **Dr. Zoltán Nemes** (Laboratory of Skin Biology, NIAMS, NIH, Bethesda, Maryland, USA) and **Dr. Zsolt Keresztessy** (home Institute), respectively. I am full of gratitute to **Prof. Dr. Carlo Bergamini** (University of Ferrara, Ferrara, Italy) for the excellent protein purification training; to **Dr. Manfred S. Weiss** (Institute of Molecular Biotechnology, Department of Structural Biology and Crystallography, Jena, Germany) for the laborious month worked together on homology modeling (thanking the possibility to the Head of Institute – **Prof. Dr. Rolf Hilgenfeld**). At the beginning of my Ph.D. years I was helped a lot by my colleagues **Dr. András Mádi** and **Dr. József Tőzser,** thanks for that**.** Many thanks to **Bruna Pucci** (Torvergata University, Rome, Italy) for the plasmid construction of non-fused TGase 2 and to **Prof. Dr. Gerry Melino** for the possibility of that. Furthermore, thanks to **Júlia Szabó** for technical assistance and to **Erika Magyar** for preparing the electron-micrographic pictures.

In addition, in especially emphasis, I owe the never-ending spiritual aiding to **my wife** and **my mother**.

12. References

1. S.Y. Kim, S.L. Chung, P.M. Steinert, J. Biol. Chem. 270 (1995) 18026-18035
2. H.J. Dubbink, N.S. Verkaik, P.W. Faber, J. Trapman, F.H. Schröder, J.C. Romijn, Biochem. J. 315 (1996) 901-908
3. D. Aeschlimann, M.K. Koeller, B.L. Allen-Hoffmann, D.F. Mosher, J. Biol. Chem. 273 (1998) 3452-3460
4. C.M. Cohen, E. Dotimas, C. Korsgren, Semin. Hematol. 30 (1993) 119-137
5. L. Muszbek, V.C. Yee, Z. Hevessy, Thromb. Res. 94 (1999) 271-305
6. M.S. Weiss, H.J. Metzner, R. Hilgenfeld, FEBS Lett. 423 (1998) 291-296
7. M.M. Sarasua, K.A. Koehler, C. Skrzynia, J.M. McDonagh, J. Biol. Chem. 257 (1982) 14102-14109
8. B.A. Fox, V.C. Yee, L.C. Pedersen, I.L. Trong, P.D. Bishop, R.E. Stenkamp, D.C. Teller, J. Biol. Chem. 274 (1999) 4917-4923
9. B.A. Lewis, J.-M. Freyssinet, J.J. Holbrook, Biochem. J. 169 (1978) 397-402
10. J. Polgar, V. Hidasi, L. Muszbek, J. Biochem. 267 (1990) 557-560
11. P.J. Bungay, R.A. Owen, I.C. Coutts, M. Griffin, Biochem J. 235 (1986) 269-278
12. P.J.A. Davies, D.R. Davies, A. Levitski, R.R. Maxfield, P. Milhaud, M.C. Willingham, I. Pastan, Nature 283 (1980) 162-167
13. L. Fesus, V. Thomazy, F. Autuory, M. P. Ceru, E. Tarcsa, M. Piacentini, FEBS Lett. 245 (1989) 150-154
14. J. Martinez, D.G. Chalupowicz, R.K. Roush, A. Sheth, C. Barsignian, Biochemistry 33 (1994) 2538-2545
15. A.E. Chiocca, J.P. Stein, P.J.A. Davies, J. Cell Biochem. 39 (1989) 293-304
16. R.N. Barnes, P.J. Bungay, B.M. Elliott, P.l. Walton, M. Griffin, Carcinogenesis 6 (1985) 459-463
17. C.R.L. Knight, R.C. Rees, M. Griffin, Biochim. Biophys. Acta 1096 (1991) 312-318
18. C. Bergamini, FEBS Lett. 239 (1988) 255-258
19. M. Signorini, P. Chiozzi, C. Bergamini, Biochem. Int. 19 (1989) 1205-1212
20. P.A. Smethurst, M. Griffin, Biochem. J. 313 (1996) 803-808
21. S.E. Iismaa, M.J. Wu, N. Nanda, W.B. Church, R.M. Graham, J. Biol. Chem. 275 (2000) 18259-18265
22. R. Casadio, E. Polverini, P. Mariani, F. Spinozzi, F. Carsughi, A. Fontana, P.P. Laureto, G. Matteucci, C.M. Bergamini, Eur. J. Biochem. 262 (1999) 672-679

23. C.M. Bergamini, M. Dean, F. Tanfani, C. Ferrari, A. Scatturin, Eur. J. Biochem. 266 (1999) 575-582
24. T. Mehrel, D. Hohl, J.A. Rothnagel, M.A. Longley, D. Bundman, C. Cheng, U. Lichti, M.E. Bisher, A.C. Steven, P.M. Steinert, S.H. Yuspa, D.R. Roop, Cell 61 (1990) 1103-1112
25. I.-G. Kim, J.J. Gorman, S.-C. Park, S.-I. Chung, P.M. Steinert, J. Biol. Chem. 268 (1993) 12682-12690
26. H. J. Vogel, T. Drakenberg, S. Forsen, (1983) in *NMR of Newly Accessible Nuclei* (Laszlo, P., Eds.) Vol. I, p 157, Academic Press, New York
27. W.H. Braunlin, T. Drankenberg, S. Forsen, Curr. Top. Bioenerg. 14 (1985) 97-147
28. T. Andersson, T. Drakenberg, S. Forsen, E. Thulin, M. Sward, J. Am. Chem. Soc. 104 (1982) 576-580
29. T. Drakenberg, S. Forsen, H. Lilja, J. Magn. Reson. 53 (1983) 412-422
30. H.J. Vogel, T. Andersson, W.H. Braunlin, T. Drankenberg, S. Forsen, Biochem. Biophys. Res. Commun. 122 (1984) 1350-1356
31. H.J. Vogel, W.H. Braunlin, J. Magn. Reson. 62 (1985) 42-50
32. H.J. Vogel, T. Drakenberg, S. Forsen, J.D.J. O`Neill, T. Hofmann, Biochemistry 24 (1985) 3870-3876
33. H.C. Marsh, P. Robertson Jr., M.E. Scott, K. A. Koehler, R.G. Hiskey, J. Biol. Chem. 254 (1979) 10268-10275
34. E.B. Brown, C.H. Pletcher, G.L. Nelsestuen, R.G. Bryant, J. Inorg. Biochem. 21 (1984) 337-343
35. T. Drakenberg, T. Andersson, S. Forsen, T. Wieloch, Biochemistry 23 (1984) 2387-2392
36. W.H. Braunlin, H.J. Vogel, T. Drakenberg, A. Benick, Biochemistry 25 (1986) 584-589
37. A. Teleman, T. Drakenberg, S. Forsen, Biochim. Biophys. Acta 873 (1986) 204-213
38. H.J. Vogel, T. Andersson, W.H. Braunlin, T. Drakenberg, S. Forsen, Biochem. Biophys. Res. Commun. 122 (1984) 1350-1356
39. Y. Ogoma, H. Kobayashi, T. Fujii, Y. Kondo, A. Hachimori, T. Shimizu, M. Hatano, Int. J. Biol. Macromol. 14 (1992) 279-286
40. E. Chiancone, T. Drakenberg, O. Teleman, S. Forsen, J. Mol. Biol. 185 (1985*)* 205-207
41. J.M. Aramini, T. Drakenberg, T. Hiraoki, Y. Ke, K. Nitta, H.J. Vogel, Biochemistry 31 (1992) 6761-6768
42. T. Shimizu, M. Hatano, Biochem. Biophys. Res. Commun. 115 (1983*)* 22-28
43. C. Johansson, P. Brodin, T. Grundstrom, S. Forsen, T. Drakenberg, Eur. J. Biochem. 202 (1991) 1283-1290
44. M. Svard, T. Drakenberg, T. Andersson, P. Fernlund, Eur. J. Biochem. 158 (1986) 373-378

45. L. Lerner, D.A. Torchia, J. Biol. Chem. 261 (1986) 12706-12714
46. P. Bayley, P. Ahlstrom, S.R. Martin, S. Forsen, Biochem. Biophys. Res. Commun.120 (1984) 185-191
47. S. Forsen, S. Linse, E. Thulin, B. Lindegard, S.R. Martin, P.M. Bayley, P. Brodin, T. Grundstrom, Eur. J. Biochem. 177 (1988) 47-52
48. J. Kordel, S. Forsen, T. Drakenberg, W.J. Chazin, Biochemistry 29 (1990) 4400-4409
49. W.H. Braunlin, T. Drakenberg, L. Nordenskiold, J. Biomol. Struct. Dynam. 10 (1992) 333-343
50. W.H. Braunlin, T. Drakenberg, L. Nordenskiold, Biopolymers 26 (1987) 1047-1062
51. W.H. Braunlin, L. Nordenskiold, T. Drakenberg, Biopolymers 28 (1989) 1339-1342
52. F.A.O. Marston, Biochem. J. 240 (1986) 1-12
53. R. Kuhelj, M. Dolinar, J. Pungercar, V. Turk, Eur. J. Biochem. 229 (1995) 533-539
54. J.L. Cleland, C. Hedgepeth, D.I.C. Wang, J. Biol. Chem. 267 (1992) 13327-13334
55. E.E. Dibella, M.C. Maurer, H.A. Scheraga, J. Biol. Chem. 270 (1995) 163-169
56. K.R. Hejnaes, S. Bajne, L. Norskov, H.H. Sorensen, J. Thomsen, L. Schaffer, A. Wollmer, L. Skriver, Protein Engineering 5 (1992) 797-806
57. S. Tandon, P.M. Horowitz, J. Biol. Chem. 262 (1987) 4486-4491
58. T.J.R. Harris, T. Patel, F.A.O. Marston, S. Little, J.S. Emtage, Mol. Biol. Med. 3 (1986) 279-292
59. Z. Nemes, L.N. Marekov, P.M. Steinert, J. Biol. Chem. 274 (1999) 11013-11021
60. H.E. Karges, H.J. Metzner, Semin. Thromb. Hemost. 22 (1996) 427-436
61. V. Gentile, M. Saydak, E.A. Chiocca, O. Akande, P.J. Birckbichler, K.N. Lee, J.P. Stein, P.J.A. Davies, J. Biol. Chem. 266 (1991) 478-483
62. V. Gentile, V. Thomazy, M. Piacentini, L. Fesüs, P.J.A. Davies, J. Cell Biol. 119 (1992) 463-474
63. S.E. Iismaa, L. Chung, M.-J. Wu, D.C. Teller, V.C. Yee, R.M. Graham, Biochemistry 36 (1997) 11655-11664
64. M.M. Bradford, Anal. Biochem. 72 (1976) 248-254
65. T.F. Slaughter, K.E. Achyuthan, T.-S. Lai, C.S. Greenberg, Anal. Biochem. 205 (1992) 166-171
66. U.K. Laemmli, Nature 227 (1970) 680-685
67. C.S. Unterkircher, S.C. Yazaki, M.T. Shimizu, A.O. Jorge, Z.P. Camargo, J. Med. Vet. Mycol. 34 (1996) 273-277
68. J. Kyhse-Andersen, J. Biochem. Biophys. Methods 10 (1984) 203-209

69. K.J. Neurohr, T. Drakenberg, S. Forsen, NMR of Newly Accessible Nuclei, Academic, New York, Vol. 2, 229-251, 1983
70. C. Bergamini, M. Signori, Biochem. J. 291 (1993) 37-39
71. J. Devereux, P. Haeberli, O. Smithies, Nucl. Acids. Res. 12 (1984) 387-395
72. W.R. Pearson, D.J. Lipman, Proc. Natl.Acad. Sci. USA 85 (1988) 2444-2448
73. D. Fischer, D. Eisenberg, Protein Science 5 (1996) 947-955
74. T.A. Jones, J.-Y. Zou, S.W. Cowan, M. Kjeldgaard, Acta Cryst. A47 (1991) 110-119
75. A.T. Brunger, J. Kuriyan, M. Karplus, Science 235 (1987) 458-460
76. Collaborative Computational Project Number 4, Acta Cryst. D50, 760-763, 1994
77. R.A. Laskowski, M.W. MacArthur, D.S. Moss, J.M. Thornton, J. Appl. Cryst. 26 (1993) 283-291
78. A. Nicholls, K. Sharp, B. Honig, Proteins, Structure, Function and Genetics, Vol. 11, No.4, p. 281ff, 1991
79. T-S. Lai, T.F. Slaughter, K.A. Peoples, J.M. Hettasch, C.S. Greenberg, J. Biol. Chem. 273 (1998) 1776-1781
80. M. Holz, Prog. NMR Spectrosc. 18 (1985) 327-423
81. W.J. O`Sullivan, D.D. Perrin, Biochemistry 3 (1963) 18-26
82. L. Helm, H.G. Hertz Z. Phys. Chem. Neue Folge 127 (1981) 23-44
83. R. Casadio, E. Polverini, P. Mariani, F. Spinozzi, F. Carsughi, A. Fontana, P.P. Laureto, G. Matteucci, C.M. Bergamini, Eur. J. Biochem. 262 (1999) 672-679
84. A. Monsonego, I. Friedmann, Y. Shasni, M. Eisenstein, M. Schwartz, J. Mol. Biol. 282 (1998) 713-720
85. S.E. Iismaa, L. Chung, M.-J. Wu, D.C. Teller, V.C. Yee, R.M. Graham, Biochemistry 36 (1997) 11655-11664
86. K. Nakanishi, K. Nara, H. Hagiwara, Y. Aoyama, H. Ueno, S. Hirose, Eur. J. Biochem. 202 (1991) 15-21
87. K. Noguchi, K. Ishikawa, Ki. Yokoyama, T. Ohtsuka, N. Nio, E. Suzuki., J Biol Chem 276 (2001) 12055-12059
88. T.-S. Lai, T.F. Slaughter, C.M. Koropchak, Z.A. Haroon, C.S. Greenberg, J. Biol. Chem. 271 (1996) 31191-31195
89. S.N.P. Murthy, L. Lorand, Proc. Natl. Acad. Sci. USA 97 (2000) 7744-7747
90. M.S. Weiss, R. Hilgenfeld, Acta Cryst., D55 (1999) 1858-1862

13. PUBLICATIONS

13.1. Papers this thesis is based on

Attila Ambrus and László Fésüs (2001) Polyethylene glycol enhanced refolding of the recombinant human tissue transglutaminase. Prep. Biochem. &Biotechnol. 31(1) 59-70 (2001) IF: 0.447.

Attila Ambrus, István Bányai, Manfred Weiss, Rolf Hilgenfeld, László Muszbek, Zsolt Keresztessy and László Fésüs, Calcium binding of transglutaminases: a ^{43}Ca NMR study combined with surface polarity analysis. J Biomol Struct Dyn (in press) IF: 1.643

ΣIF: 2.090

13.2. Posters

Attila Ambrus, L. Fésüs (1999) Structural investigations of human tissue transglutaminase. 4th Work-meeting of the Molecular Biology Section of the Hungarian Biochemical Society, Eger, Hungary, Abstract No. DP-1, p.66.

Attila Ambrus, István Bányai, Manfred Weiss, Rolf Hilgenfeld, László Muszbek, Zsolt Keresztessy, László Fésüs (2000) Calcium binding of transglutaminases: a ^{43}Ca NMR study combined with surface polarity analysis. Sixth International Transglutaminase Conference, Lyon, France, Abstract No. 1.

Attila Ambrus, István Bányai, Manfred Weiss, Rolf Hilgenfeld, László Muszbek, Zsolt Keresztessy, László Fésüs (2000) Calcium binding of transglutaminases: a ^{43}Ca NMR study combined with surface polarity analysis. “The present students – the future scientists”, The Day of Science, Budapest, Hungary, Abstract No.: 12.

13.3. Other Papers

Ambrus Attila, Batta Gyula, Kövér E. Katalin, Examination of the structure of Calretinin: Backbone assignment and secondary structure elements of domain I-II. Biokémia (in press) IF: -.

Małgorzata Palczewska, Attila Ambrus, Patrick Groves, Gyula Batta, Katalin E. Kövér, Werner Klaus, Agata Kaleta and Jacek Kuźnicki, Calcium-dependent properties of neuronal calretinin modules I-II (residues 1-100) differ from those of homologous calbindin D_{28k} modules I-II (residues 1-93). (manuscript in preparation).

Imre Tóth, Attila Ambrus and Istvan Bányai, On the mechanism of cyanide substitution of $Tl(EDTA)CN^{2-}$ complex. (manuscript in preparation).

Attila Ambrus and István Bányai, Study of deuterium isotope effect in proton exchange reaction of HCN. (manuscript in preparation).

Gyula Batta, Attila Ambrus, Patrick Groves and Jacek Kuznicki, Backbone assignment and secondary structure elements of the calcium-dependent neuronal calretinin modules I-II (residues 1-100), (manuscript in preparation).

13.4. Other Posters

Batta Gyula, Ambrus Attila, E. Kövér Katalin, Patrick Groves, Malgorzata Palczewska, Jacek Kuznicki (2000) NMR assignment and dynamic examination of Calretinin protein modules I-II. Conference of Chemists 2000, Debrecen, Hungary.

Batta, G., Ambrus, A., Kövér, K.E., Groves, P., Palczewska, M. and Kuznicki, J. (2000) The first (CR I-II) domain of Calretinin, a neuronal calcium binding protein. XIX. International Conference on Magnetic Resonance in Biological Systems, Florence, Italy, Abstract: p. 122 (top).

Batta Gyula, Ambrus Attila, E. Kövér Katalin, Patrick Groves, Malgorzata Palczewska, Jacek Kuznicki (2000) NMR assignment and dynamic examination of Calretinin protein modules I-II. "The present students – the future scientists", The Day of Science, Budapest, Hungary, Abstract No.: 13.